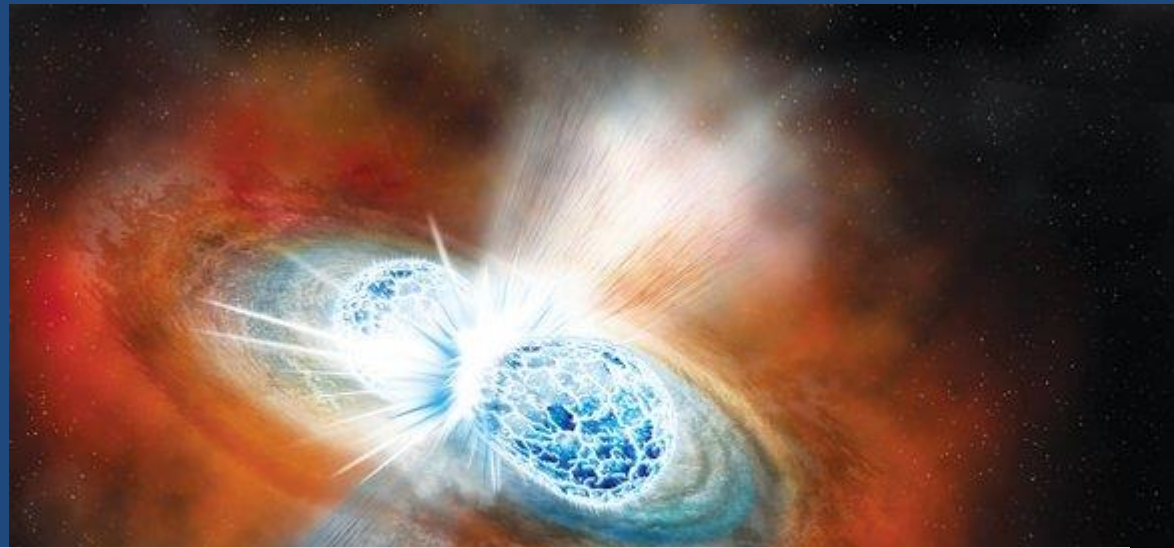
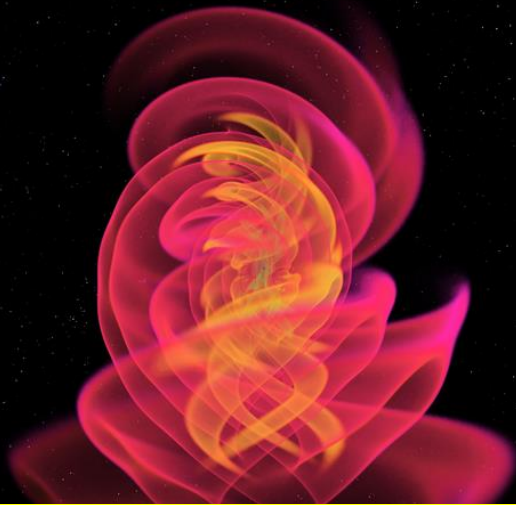


Konstantin Postnov
Sternberg Astronomical
Institute, Moscow U.



Gravitational waves: Astrophysical and cosmological inferences



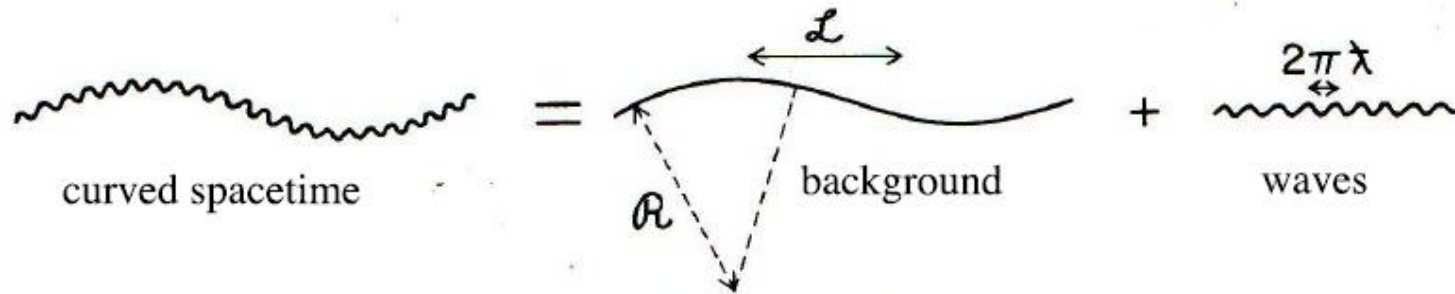
International Conference on Quantum Field Theory, High-Energy Physics, and Cosmology

Plan

- Introduction
- 10-1000 Hz: ground-based laser interferometers
- LIGO/Virgo O1-O3
- Astrophysical implications
- NanoHz: pulsar timing arrays results

Gravitational waves

$$g_{\alpha\beta} = g_{\alpha\beta}^{\text{B}} + h_{\alpha\beta}, \quad R_{\alpha\beta\gamma\delta} = R_{\alpha\beta\gamma\delta}^{\text{B}}$$



$$\square \bar{h}_{\mu\nu} = -\frac{16\pi G}{c^4} T_{\mu\nu} \quad \partial^\nu \bar{h}_{\mu\nu} = 0.$$

GW energy flux

- Energy density

$$t^{00} = \frac{c^2}{16\pi G} \langle \dot{h}_+^2 + \dot{h}_\times^2 \rangle$$

- Power

$$\frac{dE_{\text{GW}}}{dt} = \frac{c^3 r^2}{16\pi G} \int d\Omega \langle \dot{h}_+^2 + \dot{h}_\times^2 \rangle.$$

- Flux

$$T^{\text{GW } 0z} \simeq \frac{\pi c^3}{4 G} f^2 h_{\text{amp}}^2 \simeq 300 \frac{\text{ergs}}{\text{cm}^2 \text{ sec}} \left(\frac{f}{1 \text{ kHz}} \right)^2 \left(\frac{h_{\text{amp}}}{10^{-21}} \right)^2$$

GW emission

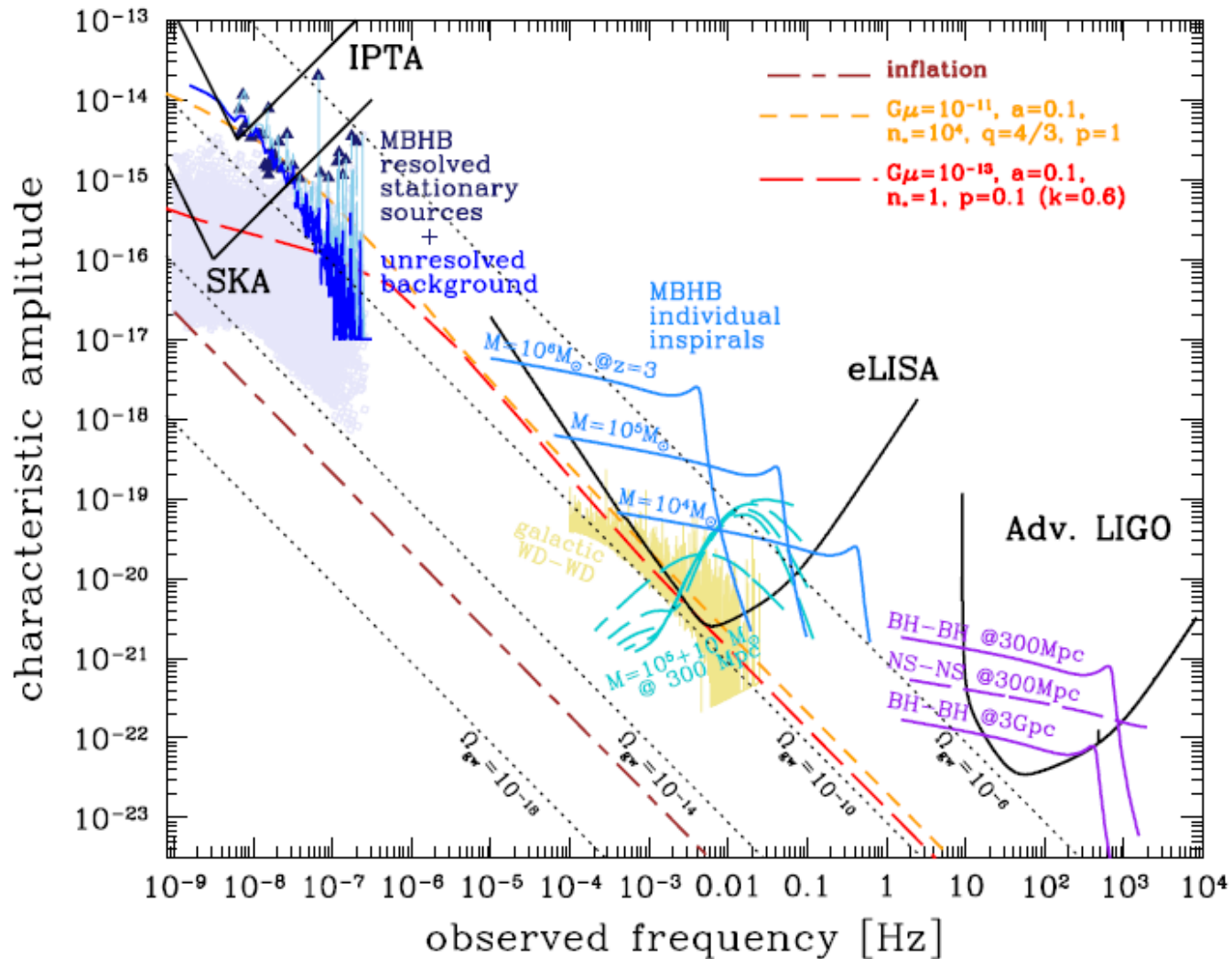
$$\bar{h}_{\mu\nu}(t, \mathbf{x}) = -4 \frac{G}{c^2} \int_{\mathcal{V}} \frac{T_{\mu\nu}(t - |\mathbf{x} - \mathbf{x}'|/c, \mathbf{x}')}{|\mathbf{x} - \mathbf{x}'|} d^3\mathbf{x}'$$

- Quadrupole radiation for $v/c \ll 1$:

$$h_{jk}^{\text{GW}} = 2G \frac{\ddot{I}_{jk}}{r} \sim G \frac{\omega^2 (ML^2)}{r} \sim G \frac{E_{\text{kin}}/c^2}{r}$$

$$h_{jk}^{\text{GW}} \sim h_+ \sim h_{\times} \sim 10^{-21} \left(\frac{E_{\text{kin}}}{M_{\odot} c^2} \right) \left(\frac{100 \text{Mpc}}{r} \right)$$

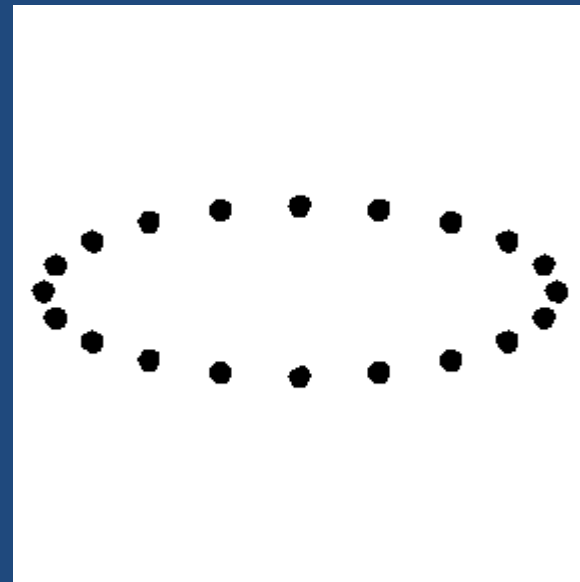
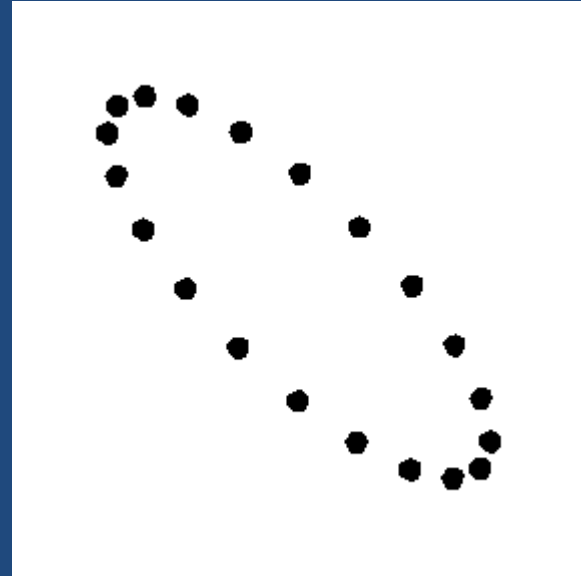
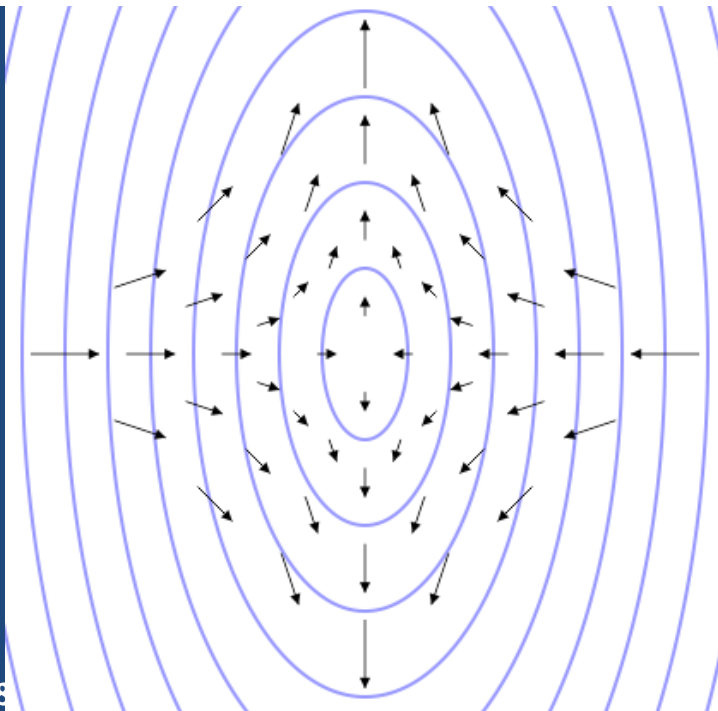
Astrophysical sources



GW produces tidal field

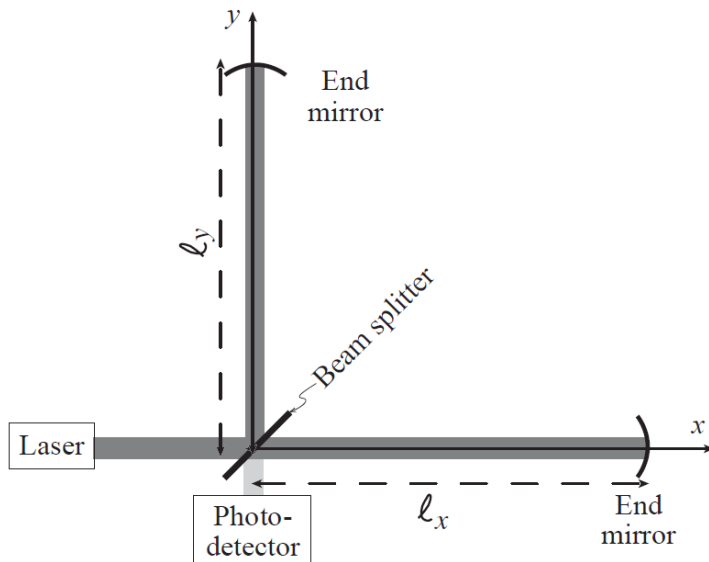
$$\mathcal{E}_{ij} = R_{i0j0} = -\frac{1}{2}\ddot{h}_{ij}^{\text{TT}}$$

$$h_{ij}^{\text{TT}} \equiv -2 \int dt \int dt \mathcal{E}_{ij}$$



Laser interferometers

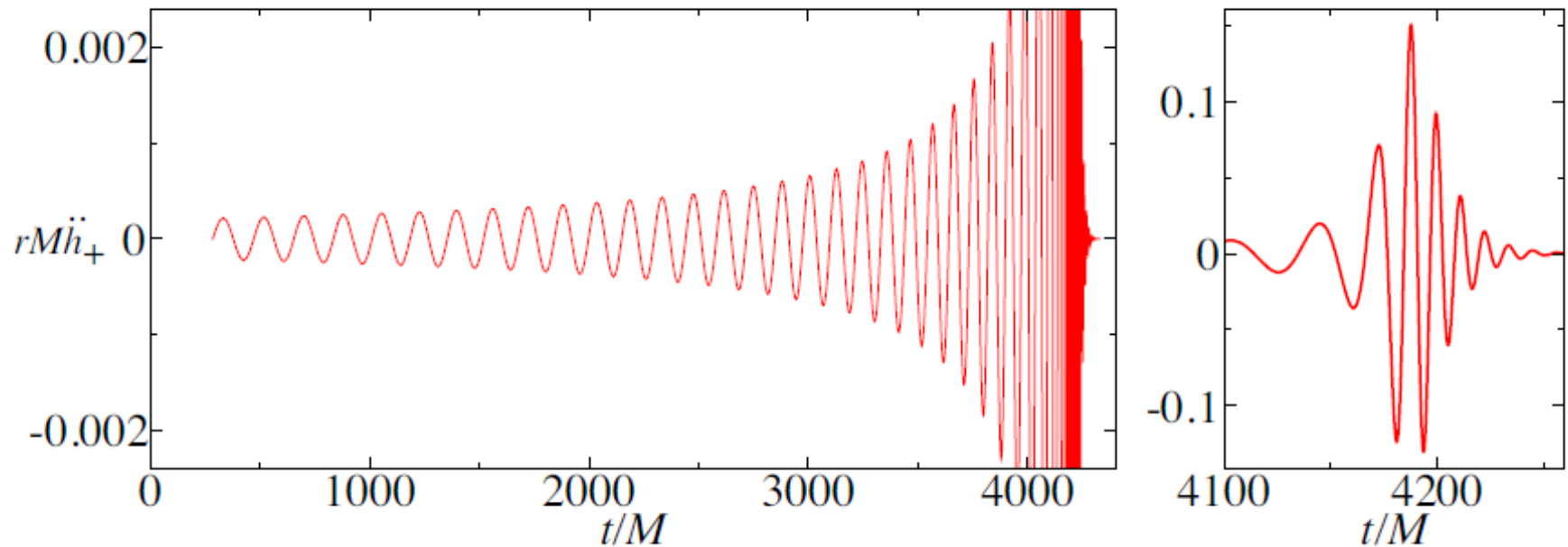
LIGO 1990-2017 ~690 MUSD



18.07.2022

Dubna-2022

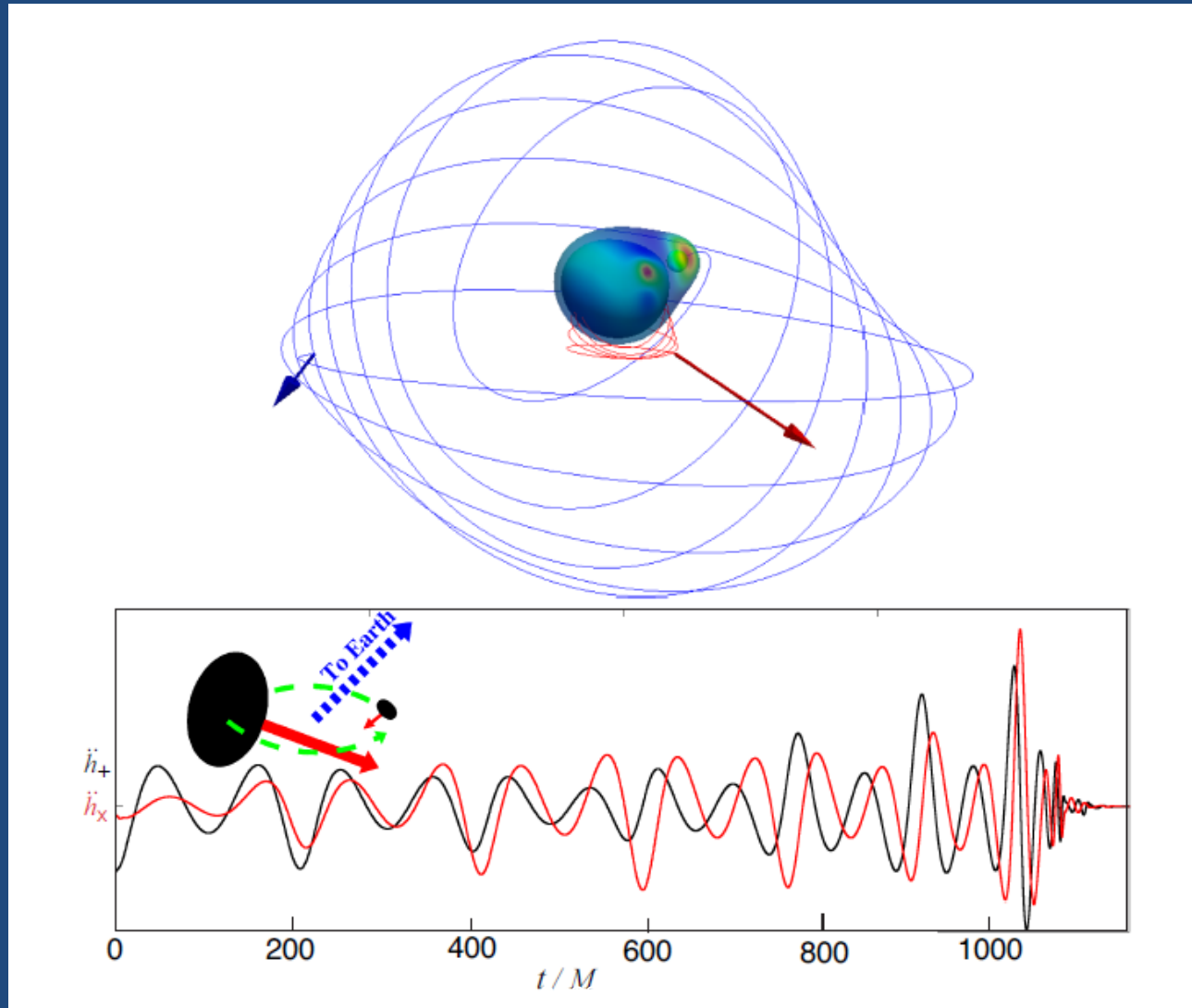
Chirp signal from coalescing binary system



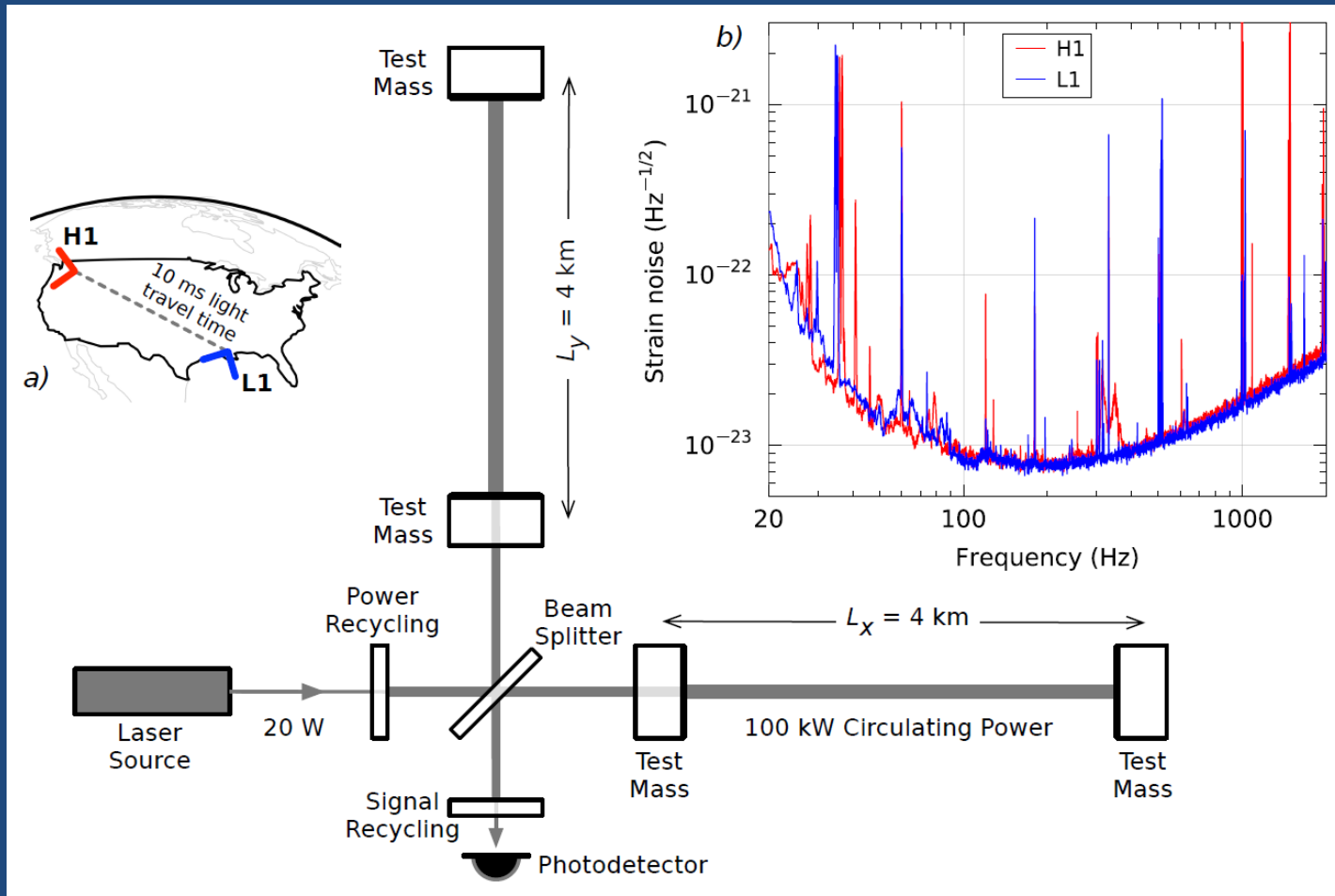
$$h_+ = h_{\hat{\theta}\hat{\theta}}^{\text{TT}} = \frac{2}{r} [\ddot{I}_{\hat{\theta}\hat{\theta}}(t-r)]^{\text{TT}} = -2(1 + \cos^2 \theta) \frac{\mu(M\Omega)^{2/3}}{r} \cos[2(\Omega t - \Omega r - \phi)]$$

$$h_\times = h_{\hat{\theta}\hat{\phi}}^{\text{TT}} = \frac{2}{r} [\ddot{I}_{\hat{\theta}\hat{\phi}}(t-r)]^{\text{TT}} = -4 \cos \theta \frac{\mu(M\Omega)^{2/3}}{r} \sin[2(\Omega t - \Omega r - \phi)] .$$

GW from inspiraling binary BH



LIGO



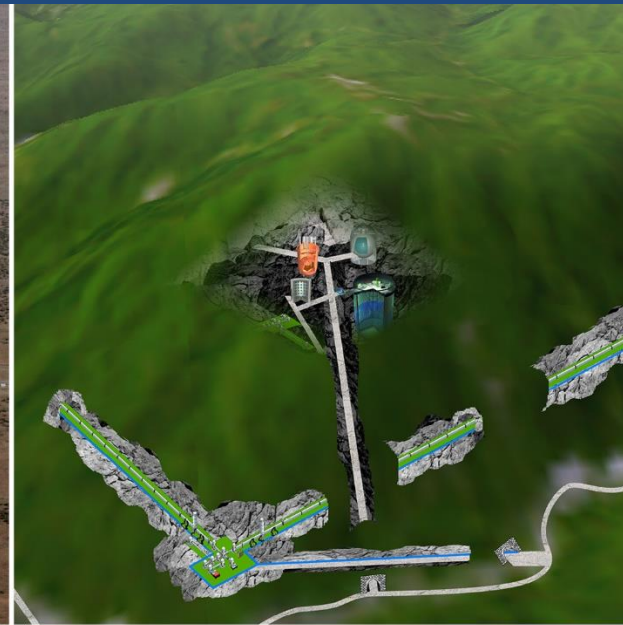
Working GW-interferometers



LIGO
Hanford
USA



KAGRA
Kamioka
Japan



Virgo
Pisa
Italy



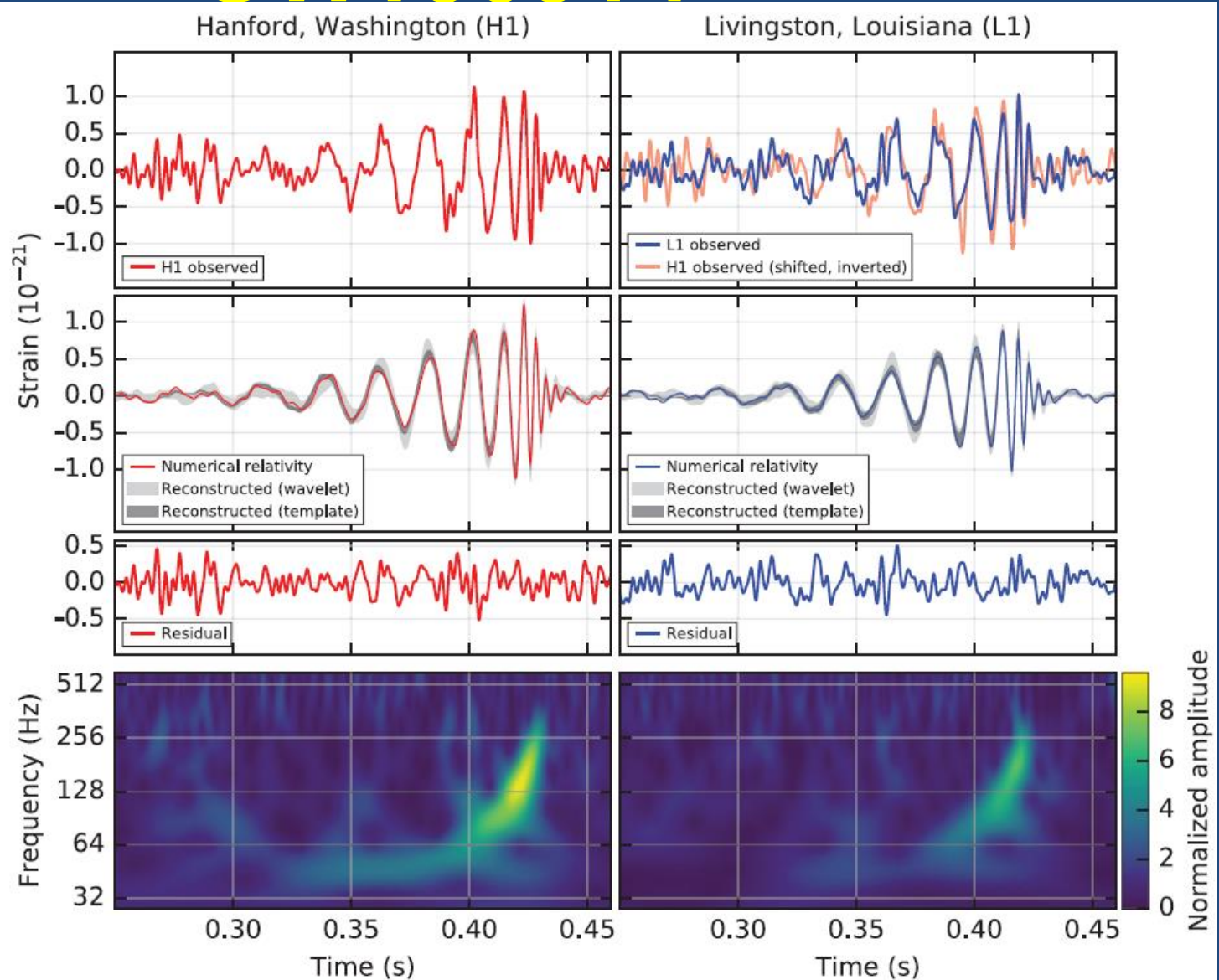
LIGO
Livingston
USA



GW150914

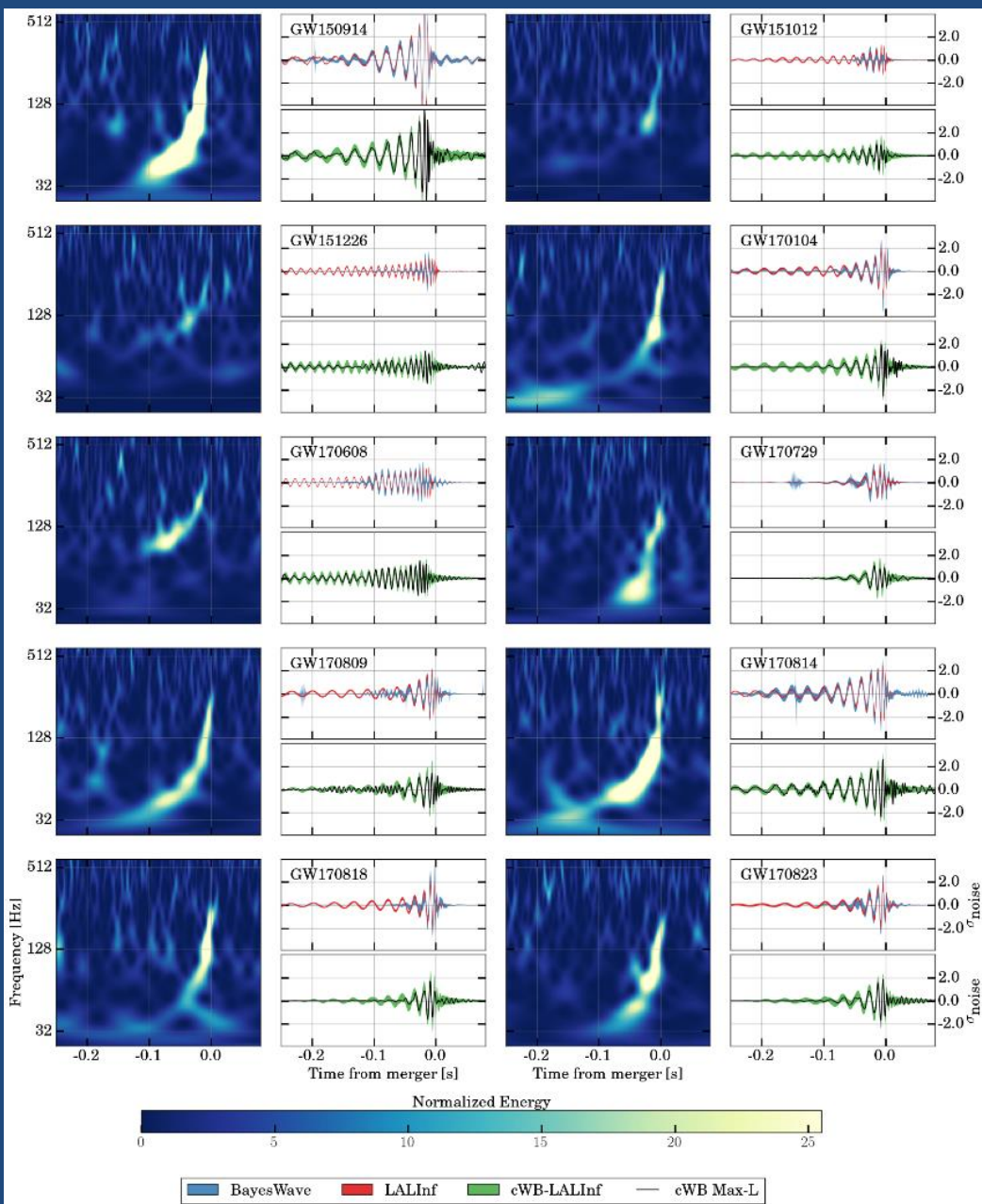
PRL 116, 061102 (2016)

35-350 Hz bandpass filter applied



Binary BHs LIGO/Virgo

GWTC-1 Catalog arXiv:1811.12907



Chirp signal from inspiraling binaries

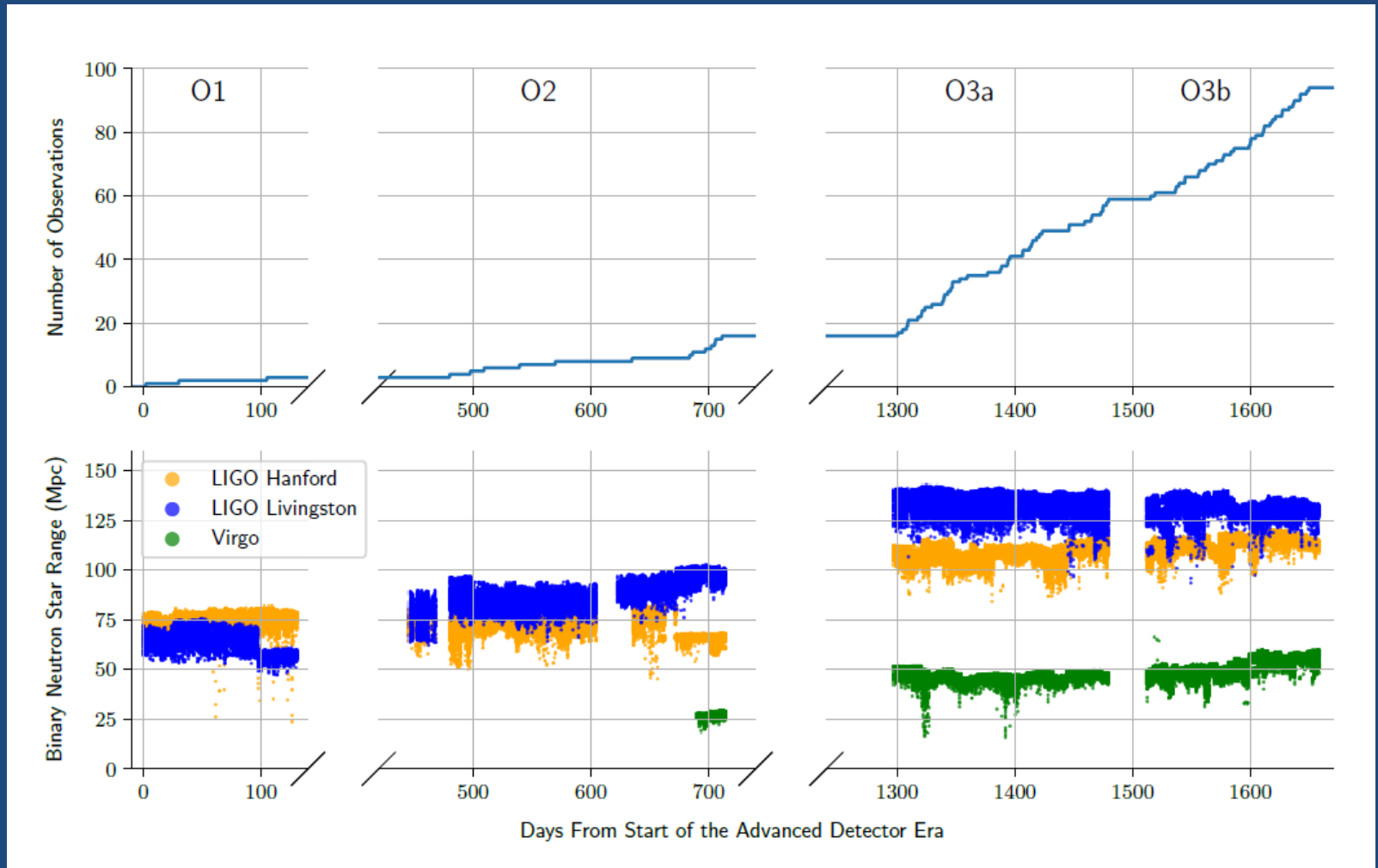
- Chirp-mass determined inspiraling signal

$$M_{ch} = (\mu^3 M^2)^{1/5}$$

$$h \sim M_{ch}^{5/3} f^{2/3} / r$$

$$\mathcal{M} = \frac{(m_1 m_2)^{3/5}}{(m_1 + m_2)^{1/5}} = \frac{c^3}{G} \left(\frac{5}{96} \pi^{-8/3} f^{-11/3} \dot{f} \right)^{3/5}$$

Chirp mass determines detection horizon. $h_{\text{lim}} \sim M^{(5/6)}$



Mass-redshift degeneracy

$$f_o = f / (1 + z), \quad dt_o = dt(1 + z)$$

$$\left. \frac{df}{dt} \right|_o = \frac{df}{dt} \frac{1}{(1 + z)^2}$$

$$M_{ch}|_o = \left(\frac{5 f_o^{-11/3} (df_o / dt)}{96 \pi^{8/3}} \right)^{3/5} = M_{ch} (1 + z) \implies f M_{ch} = inv$$

$$h_o \sim \frac{M_{ch}}{d_m} (\pi f M_{ch})^{2/3}$$

$$d_o \sim \frac{4(M_{ch})_o}{h_o} (\pi f_o (M_{ch})_o)^{2/3} = d_m (1 + z)$$

Luminosity distance

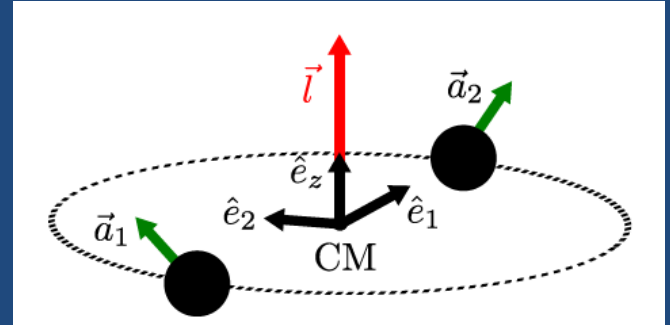
Parameters from GW observations

$$\mathcal{M} = \frac{(m_1 m_2)^{3/5}}{M^{1/5}}$$

Chirp mass

$$\chi_{\text{eff}} = \frac{(m_1 \vec{\chi}_1 + m_2 \vec{\chi}_2) \cdot \hat{L}_N}{M}$$

Effective spin

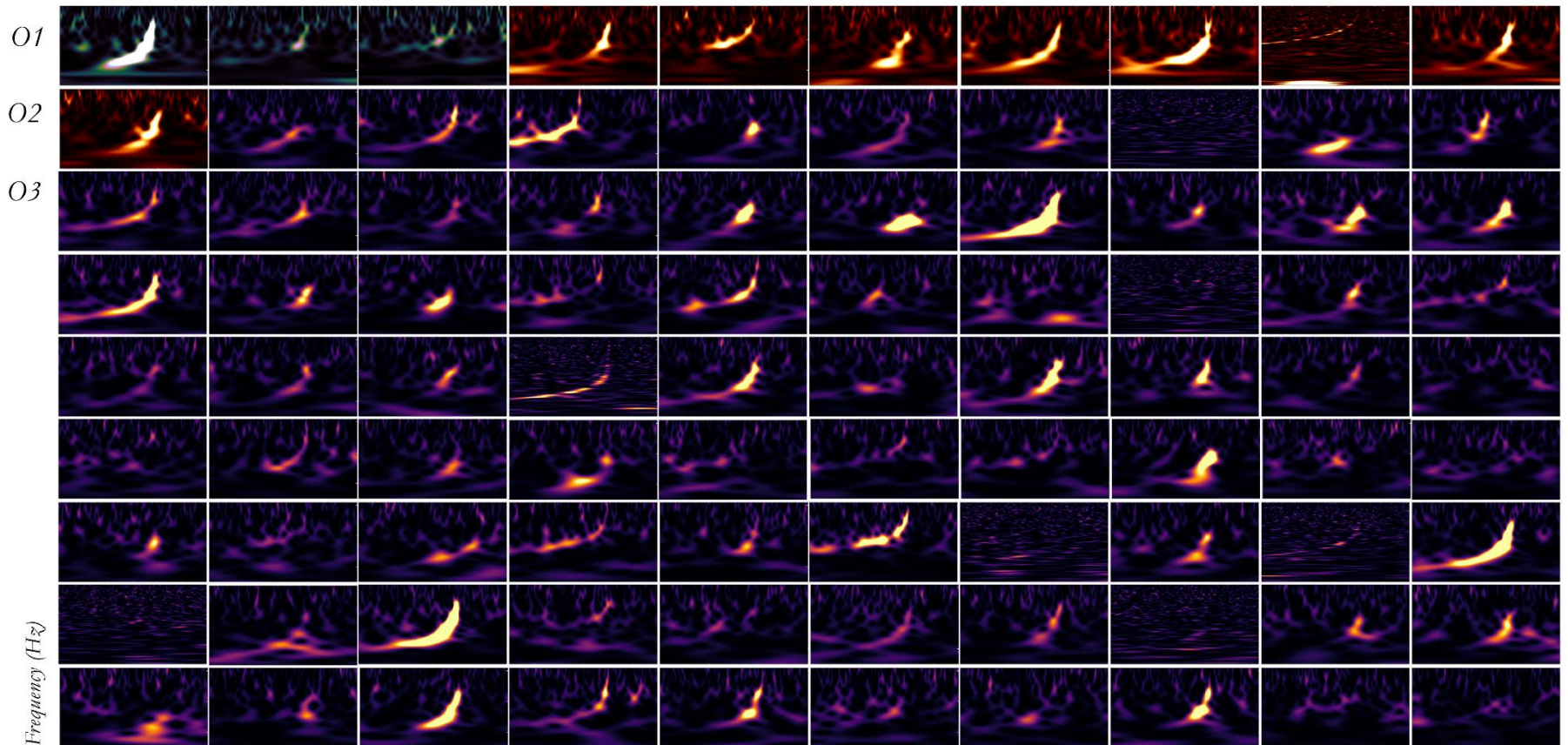


Event	m_1/M_\odot	m_2/M_\odot	\mathcal{M}/M_\odot	χ_{eff}	M_f/M_\odot	a_f	$E_{\text{rad}}/(M_\odot c^2)$	$\ell_{\text{peak}}/(\text{erg s}^{-1})$	d_L/Mpc	z	$\Delta\Omega/\text{deg}^2$
GW150914	$35.6^{+4.8}_{-3.0}$	$30.6^{+3.0}_{-4.4}$	$28.6^{+1.6}_{-1.5}$	$-0.01^{+0.12}_{-0.13}$	$63.1^{+3.3}_{-3.0}$	$0.69^{+0.05}_{-0.04}$	$3.1^{+0.4}_{-0.4}$	$3.6^{+0.4}_{-0.4} \times 10^{56}$	430^{+150}_{-170}	$0.09^{+0.03}_{-0.03}$	180
GW151012	$23.3^{+14.0}_{-5.5}$	$13.6^{+4.1}_{-4.8}$	$15.2^{+2.0}_{-1.1}$	$0.04^{+0.28}_{-0.19}$	$35.7^{+9.9}_{-3.8}$	$0.67^{+0.13}_{-0.11}$	$1.5^{+0.5}_{-0.5}$	$3.2^{+0.8}_{-1.7} \times 10^{56}$	1060^{+540}_{-480}	$0.21^{+0.09}_{-0.09}$	1555
GW151226	$13.7^{+8.8}_{-3.2}$	$7.7^{+2.2}_{-2.6}$	$8.9^{+0.3}_{-0.3}$	$0.18^{+0.20}_{-0.12}$	$20.5^{+6.4}_{-1.5}$	$0.74^{+0.07}_{-0.05}$	$1.0^{+0.1}_{-0.2}$	$3.4^{+0.7}_{-1.7} \times 10^{56}$	440^{+180}_{-190}	$0.09^{+0.04}_{-0.04}$	1033
GW170104	$31.0^{+7.2}_{-5.6}$	$20.1^{+4.9}_{-4.5}$	$21.5^{+2.1}_{-1.7}$	$-0.04^{+0.17}_{-0.20}$	$49.1^{+5.2}_{-3.9}$	$0.66^{+0.08}_{-0.10}$	$2.2^{+0.5}_{-0.5}$	$3.3^{+0.6}_{-0.9} \times 10^{56}$	960^{+430}_{-410}	$0.19^{+0.07}_{-0.08}$	924
GW170608	$10.9^{+5.3}_{-1.7}$	$7.6^{+1.3}_{-2.1}$	$7.9^{+0.2}_{-0.2}$	$0.03^{+0.19}_{-0.07}$	$17.8^{+3.2}_{-0.7}$	$0.69^{+0.04}_{-0.04}$	$0.9^{+0.05}_{-0.1}$	$3.5^{+0.4}_{-1.3} \times 10^{56}$	320^{+120}_{-110}	$0.07^{+0.02}_{-0.02}$	396
GW170729	$50.6^{+16.6}_{-10.2}$	$34.3^{+9.1}_{-10.1}$	$35.7^{+6.5}_{-4.7}$	$0.36^{+0.21}_{-0.25}$	$80.3^{+14.6}_{-10.2}$	$0.81^{+0.07}_{-0.13}$	$4.8^{+1.7}_{-1.7}$	$4.2^{+0.9}_{-1.5} \times 10^{56}$	2750^{+1350}_{-1320}	$0.48^{+0.19}_{-0.20}$	1033
GW170809	$35.2^{+8.3}_{-6.0}$	$23.8^{+5.2}_{-5.1}$	$25.0^{+2.1}_{-1.6}$	$0.07^{+0.16}_{-0.16}$	$56.4^{+5.2}_{-3.7}$	$0.70^{+0.08}_{-0.09}$	$2.7^{+0.6}_{-0.6}$	$3.5^{+0.6}_{-0.9} \times 10^{56}$	990^{+320}_{-380}	$0.20^{+0.05}_{-0.07}$	340
GW170814	$30.7^{+5.7}_{-3.0}$	$25.3^{+2.9}_{-4.1}$	$24.2^{+1.4}_{-1.1}$	$0.07^{+0.12}_{-0.11}$	$53.4^{+3.2}_{-2.4}$	$0.72^{+0.07}_{-0.05}$	$2.7^{+0.4}_{-0.3}$	$3.7^{+0.4}_{-0.5} \times 10^{56}$	580^{+160}_{-210}	$0.12^{+0.03}_{-0.04}$	87
GW170817	$1.46^{+0.12}_{-0.10}$	$1.27^{+0.09}_{-0.09}$	$1.186^{+0.001}_{-0.001}$	$0.00^{+0.02}_{-0.01}$	≤ 2.8	≤ 0.89	≥ 0.04	$\geq 0.1 \times 10^{56}$	40^{+10}_{-10}	$0.01^{+0.00}_{-0.00}$	16
GW170818	$35.5^{+7.5}_{-4.7}$	$26.8^{+4.3}_{-5.2}$	$26.7^{+2.1}_{-1.7}$	$-0.09^{+0.18}_{-0.21}$	$59.8^{+4.8}_{-3.8}$	$0.67^{+0.07}_{-0.08}$	$2.7^{+0.5}_{-0.5}$	$3.4^{+0.5}_{-0.7} \times 10^{56}$	1020^{+430}_{-360}	$0.20^{+0.07}_{-0.07}$	39
GW170823	$39.6^{+10.0}_{-6.6}$	$29.4^{+6.3}_{-7.1}$	$29.3^{+4.2}_{-3.2}$	$0.08^{+0.20}_{-0.22}$	$65.6^{+9.4}_{-6.6}$	$0.71^{+0.08}_{-0.10}$	$3.3^{+0.9}_{-0.8}$	$3.6^{+0.6}_{-0.9} \times 10^{56}$	1850^{+840}_{-840}	$0.34^{+0.13}_{-0.14}$	1651

Coalescing binaries LIGO/Virgo

Gravitational-Wave Transient Catalog

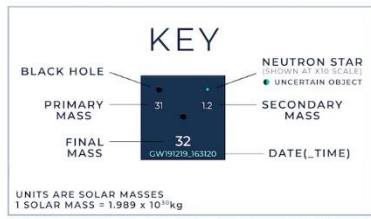
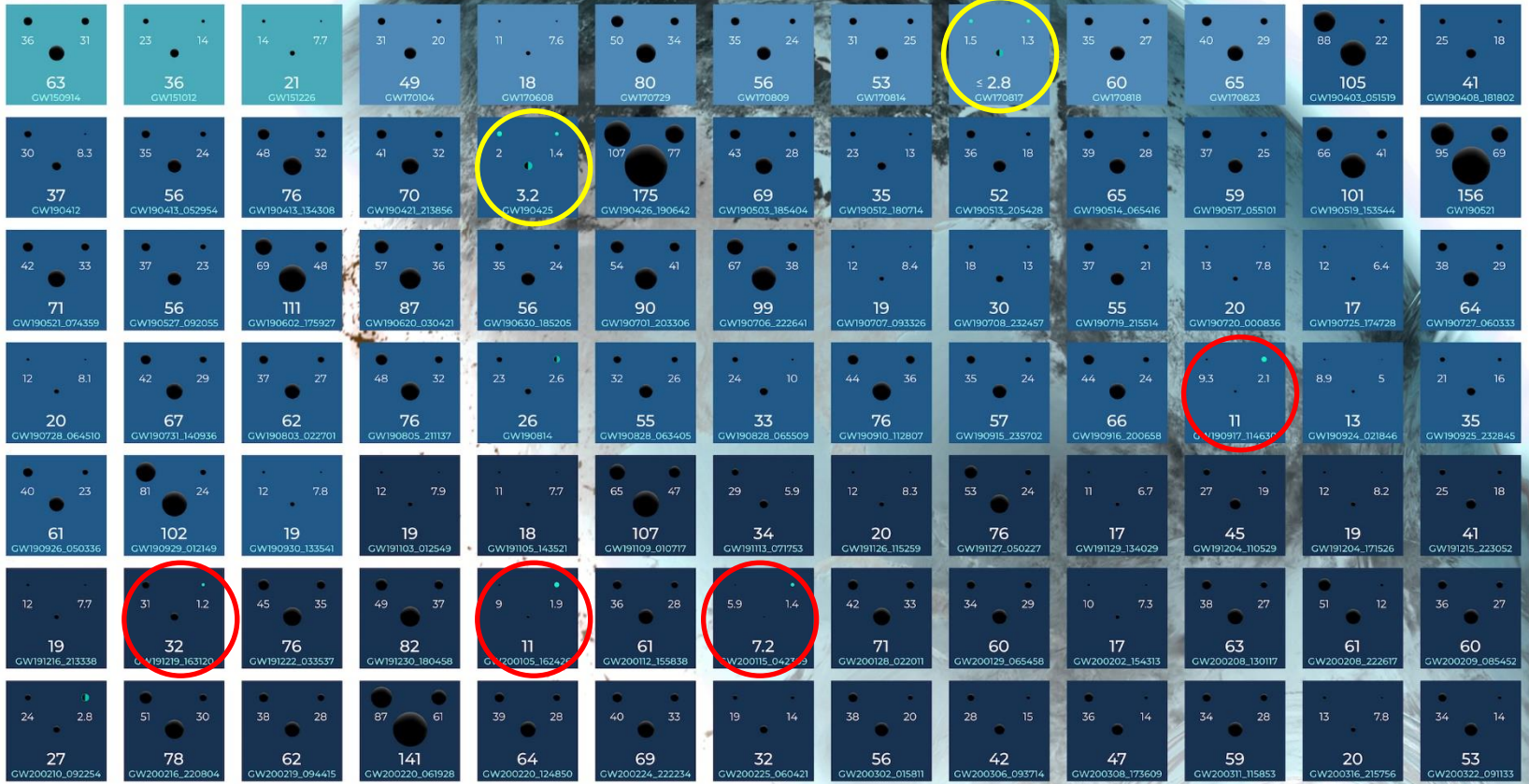
Detections from 2015-2020 of compact binaries with black holes & neutron stars



Time (s)

Sudarshan Ghonge | Karan Jani





Note that the mass estimates shown here do not include uncertainties, which is why the final mass is sometimes larger than the sum of the primary and secondary masses. In actuality, the final mass is smaller than the primary plus the secondary mass.

The events listed here have passed one of two thresholds for detection. They either have a probability of being astrophysical of at least 50%, or they pass a false alarm rate threshold of less than 1 per 3 years.

GRAVITATIONAL WAVE MERGER DETECTIONS

SINCE 2015



AIC Centre of Excellence for Gravitational Wave Discovery

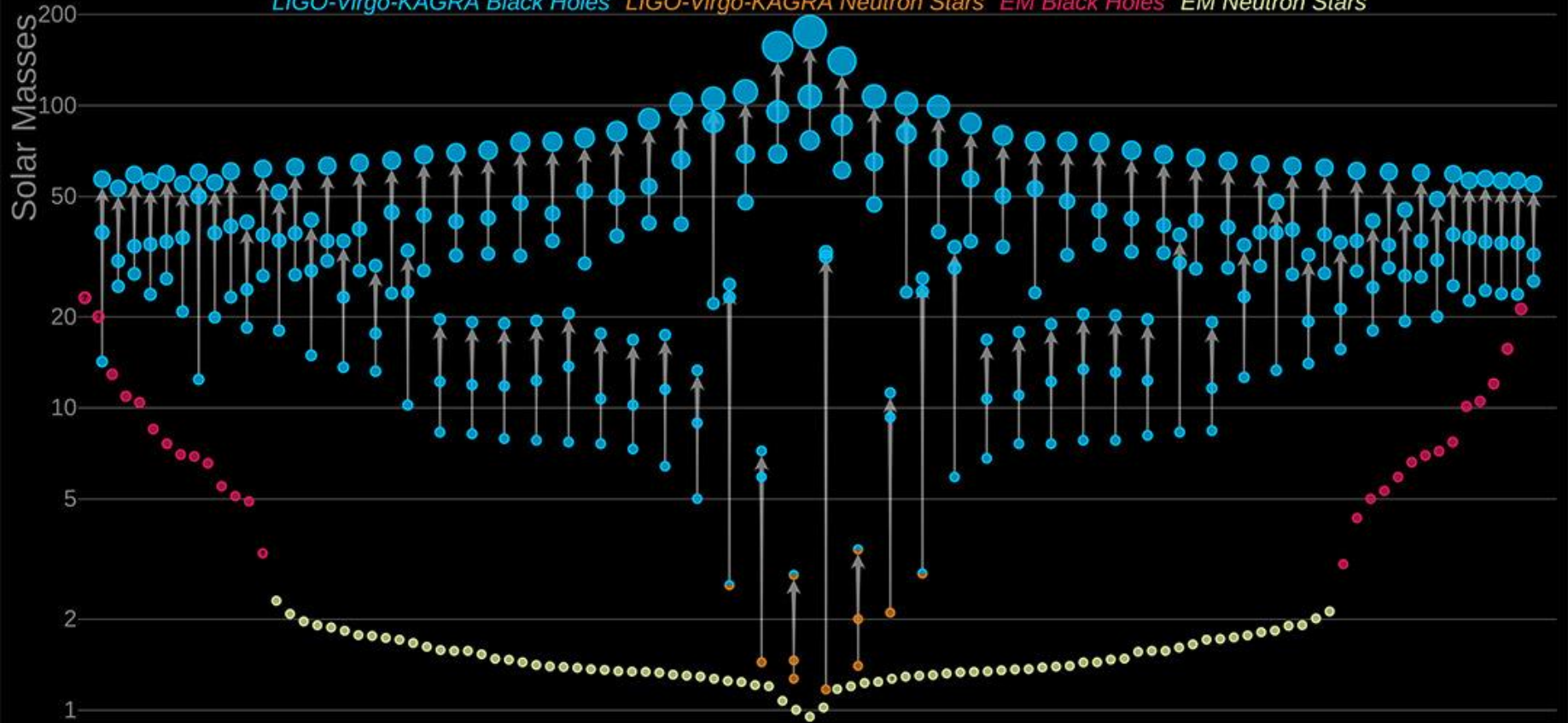


Statistical properties: summary

- O1+O2+O3: 91 robust ($S/N > 8$) detections
- Isotropic on the sky (2207.05792)
- Signal properties in agreement with GR up to a few % accuracy
- 2 NS+NS mergings, EM from GW 170817
- 4 BH+NS candidates. No electromagnetic signals.

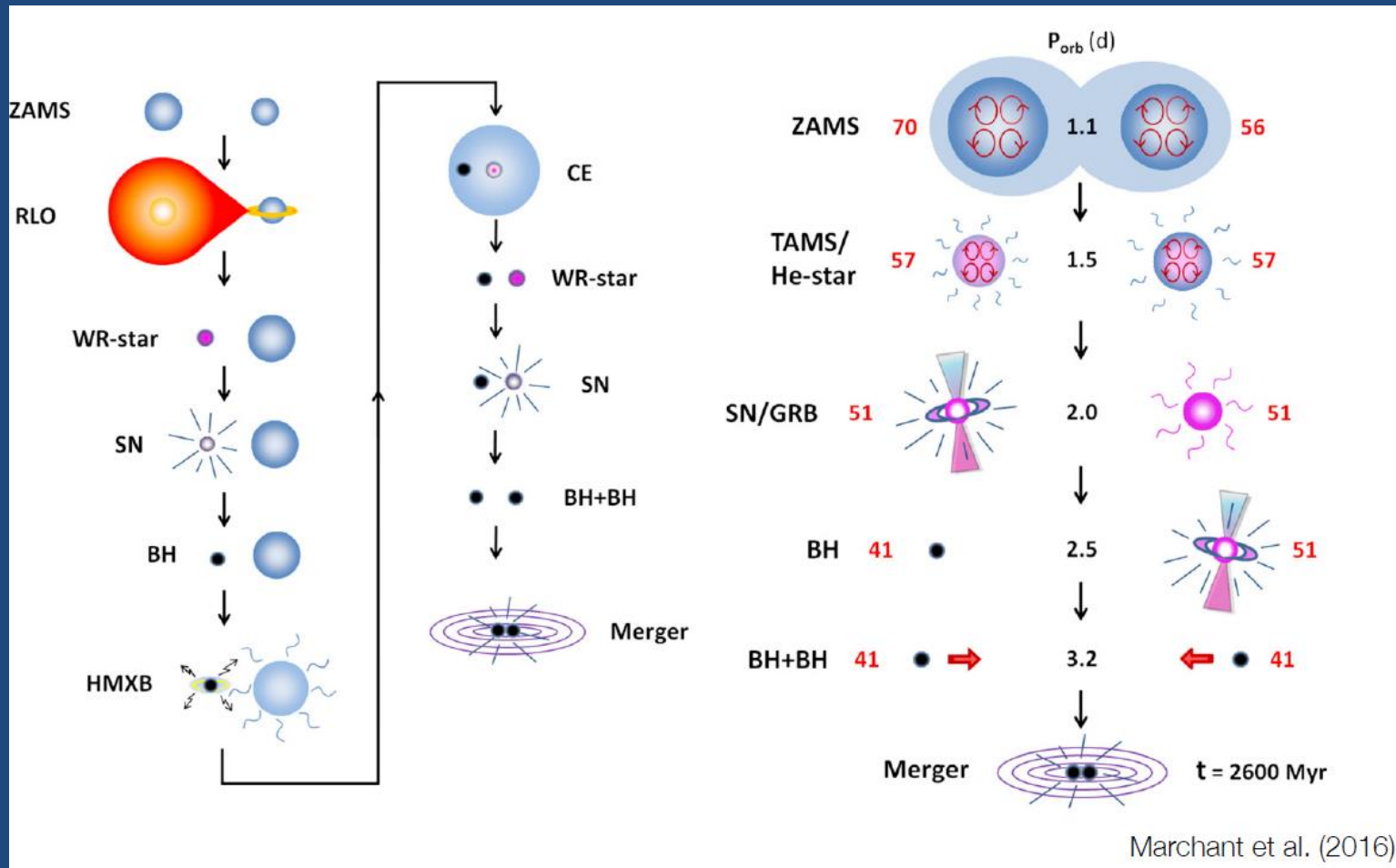
Masses in the Stellar Graveyard

LIGO-Virgo-KAGRA Black Holes LIGO-Virgo-KAGRA Neutron Stars EM Black Holes EM Neutron Stars



LIGO-Virgo-KAGRA | Aaron Geller | Northwestern

Simplest scenario: BH+BH from massive star evolution



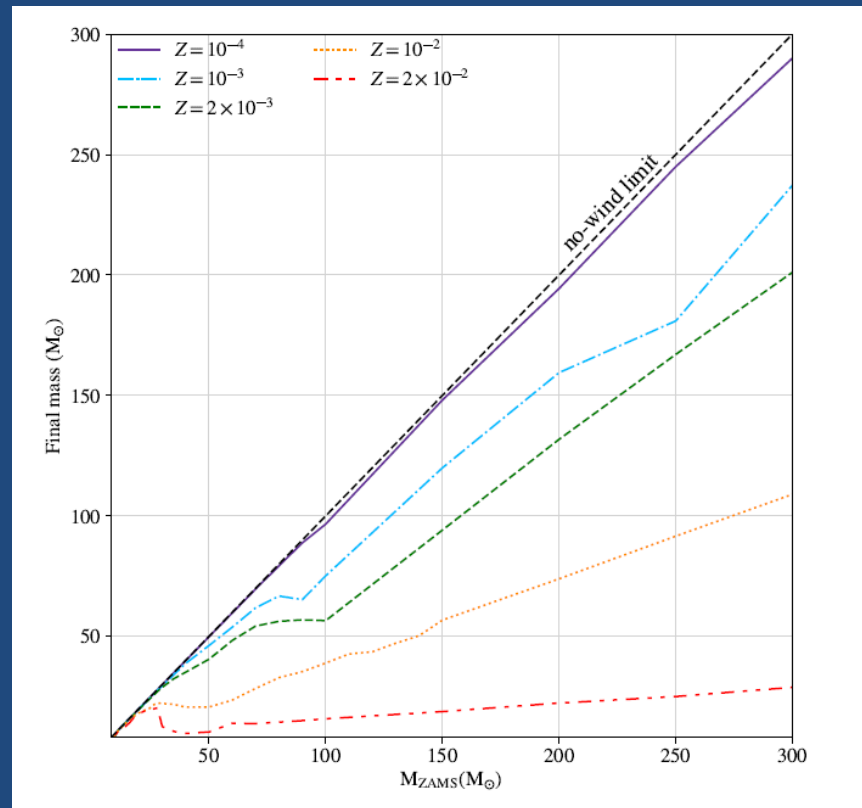
Astrophysical issues:

BH from stellar collapses, binary BH formation

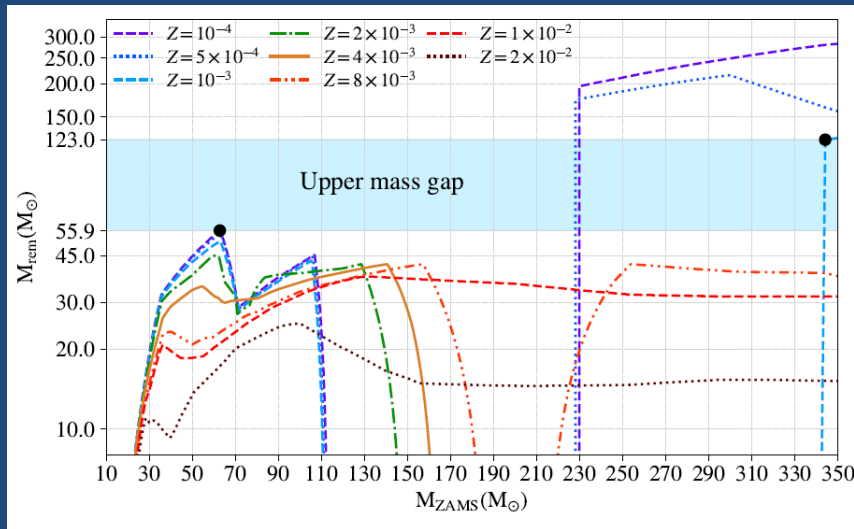
- Mass loss from massive stars
- BH mass gaps (2.5-5, 60-130 M_{sun})
- BH kicks
- BH spins
- ...

Wind mass-loss

Low metallicity is required to have no severe mass loss



Pair-instability SN (PISN) mass gap

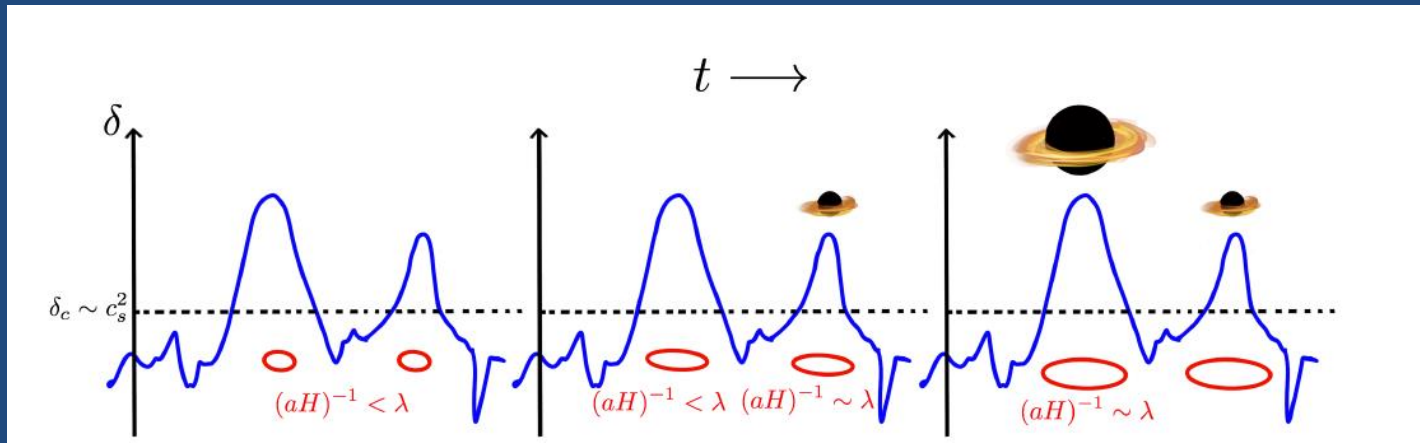


- $T_c > 7 \times 10^8 \text{K} \rightarrow \gamma + \gamma \rightarrow e^+ e^-$
- He cores $34\text{-}64 M_{\text{sun}}$ – pulsational pair instability (PPISN) with large mass loss, $64\text{-}130 M_{\text{sun}}$ – stellar explosion without remnant; $M_{\text{He}} > 130 M_{\text{sun}}$ – direct collapse to BH
- Pop III stars \rightarrow up to $85 M_{\text{sun}}$

Other scenarios

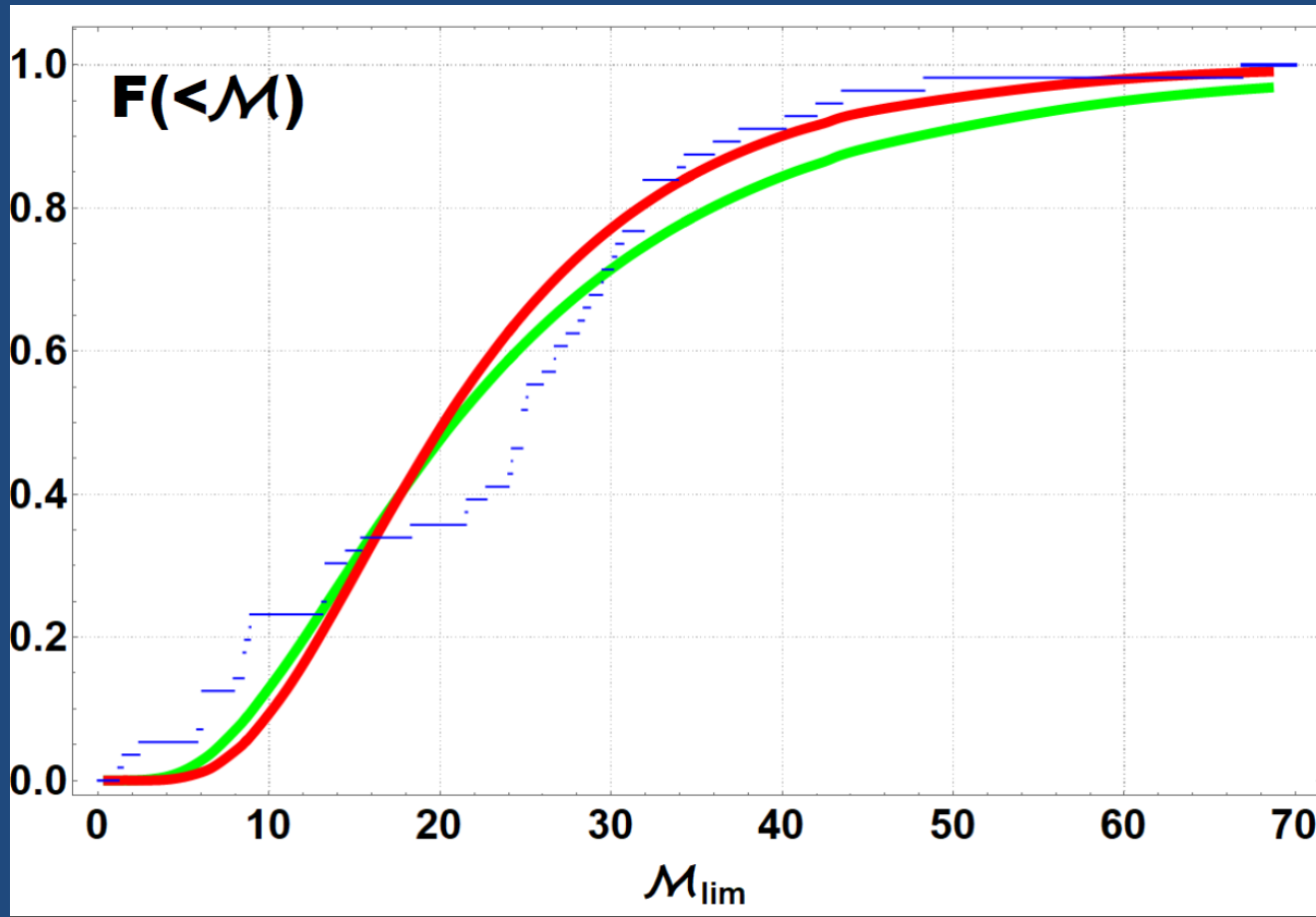
Dynamical capture in dens stellar clusters (can produce BH with $M > 50$ and non-parallel BH spins)

- “Exotic” scenarios – primordial BH
(Zeldovich, Novikov 1967... Carr 1975... Dolgov & Silk 1993...)



Example: log-normal PBH mass function GWTC1+GWTC2

$$F(M) = A \exp[-\gamma \ln^2(M/M_0)]$$



$$\gamma = 0.7, M_0 = 19$$

$$DR(M_{ch})dM_{ch} \sim A e^{-B \ln^2\left(\frac{M_{ch}}{M_0}\right)} dM_{ch}$$

Dolgov+'19

Exceptional BHBH mergers

- **GW 190814**, $M_1=26$, $q=0.112$, $M_2=2.6$ in lower mass gap? NS? Strange quark star? Outlier population? Formation from a triple star? Formation in AGN disk? Primordial BH?
- **GW190521** $m_1 = 85^{+21}_{-14} M_\odot$ $m_2 = 66^{+17}_{-18} M_\odot$ in upper mass gap (60-120), large effective spin ($\chi_{1,2} \sim 0.1-0.9$)
(Or even $m_1 = 168^{+15}_{-61} M_\odot$ $m_2 = 66^{+33}_{-3} M_\odot$??)

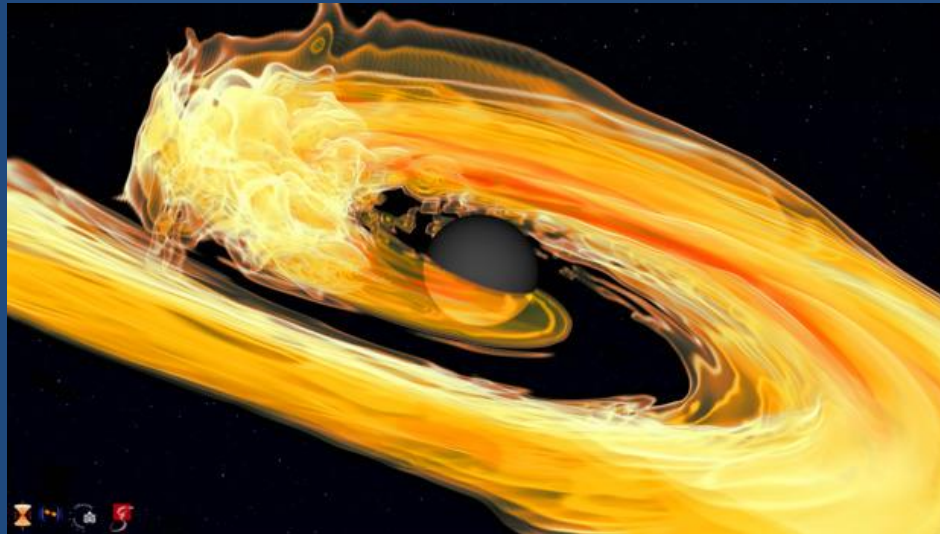
Repeated mergers in stellar clusters or AGN disks?? Primordial BH?

- **GW190412** $m_1 = 30.1^{+4.6}_{-5.3} M_\odot$ $m_2 = 8.3^{+1.6}_{-0.9} M_\odot$ high spin $\chi_1 = 0.44^{+0.16}_{-0.22}$

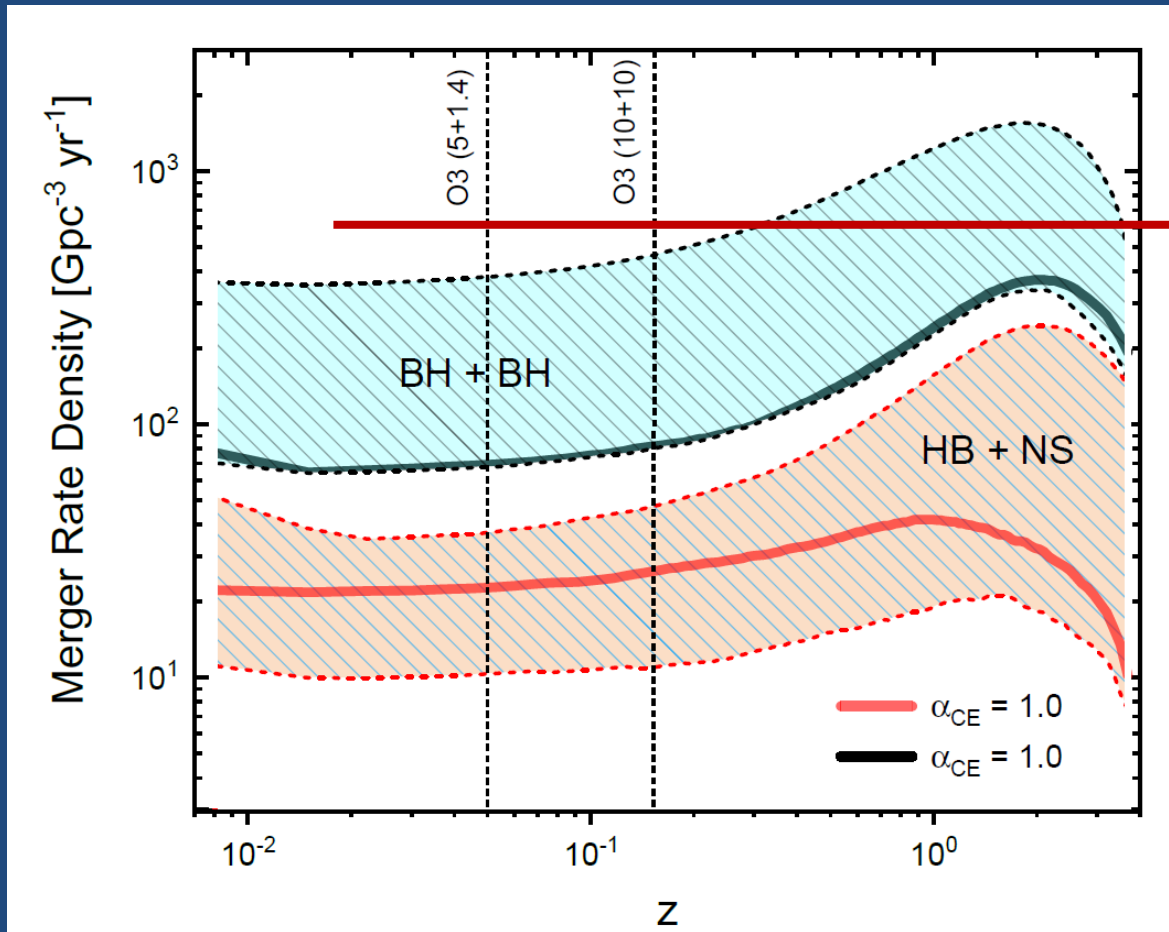
→ Hierarchical merger?

NSBH mergers

- GW 200105_1162426 (8.9+1.9)
- GW 299115_042309 (5.4+1.5) $\chi_{\text{eff}} = -0.19^{+0.23}_{-0.35}$??



Predictions from binary star evolution

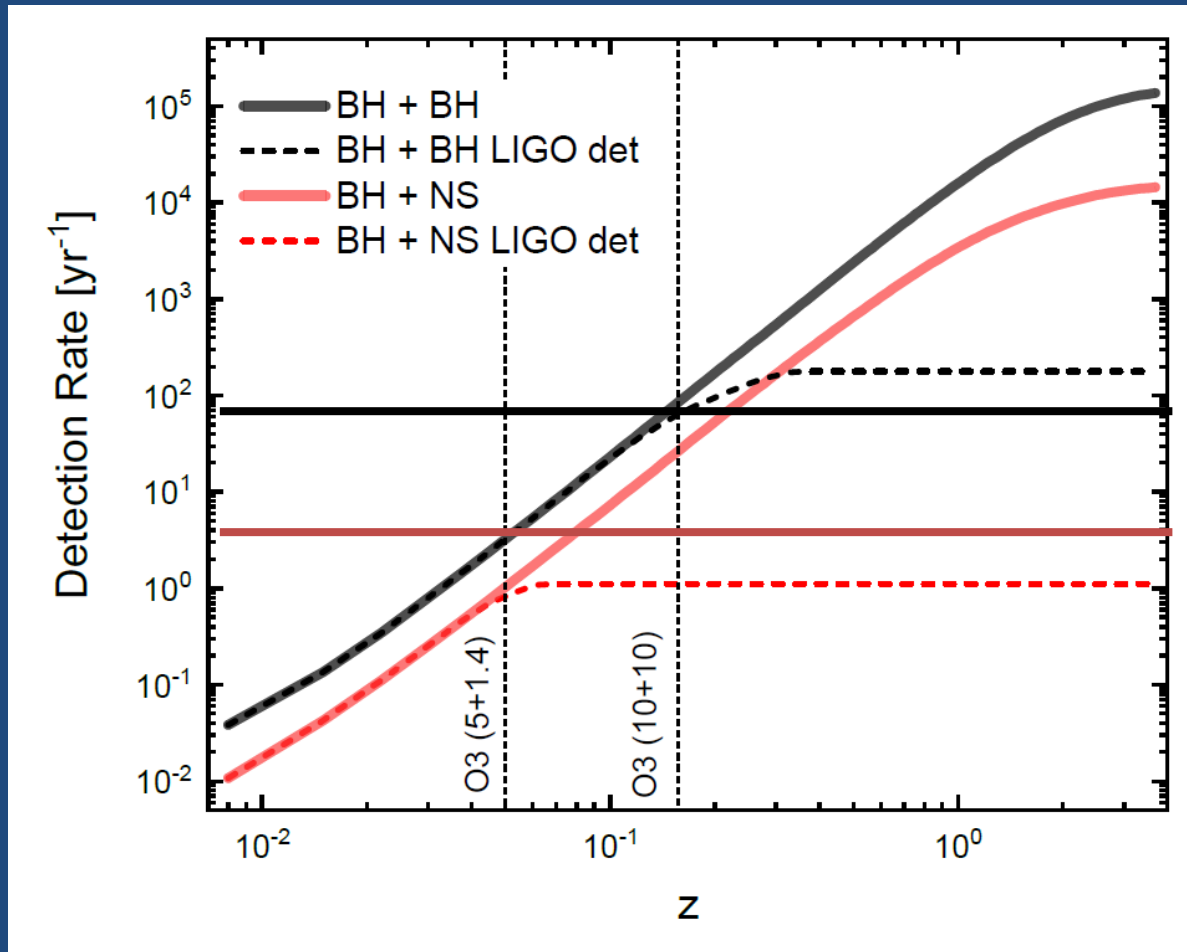


NS+BH upper limit
 $610 \text{ Gpc}^{-3} \text{ yr}^{-1}$

1811.12907

PK+ 2019; 1907.04218

Detection rate BH+BH, BH+NS

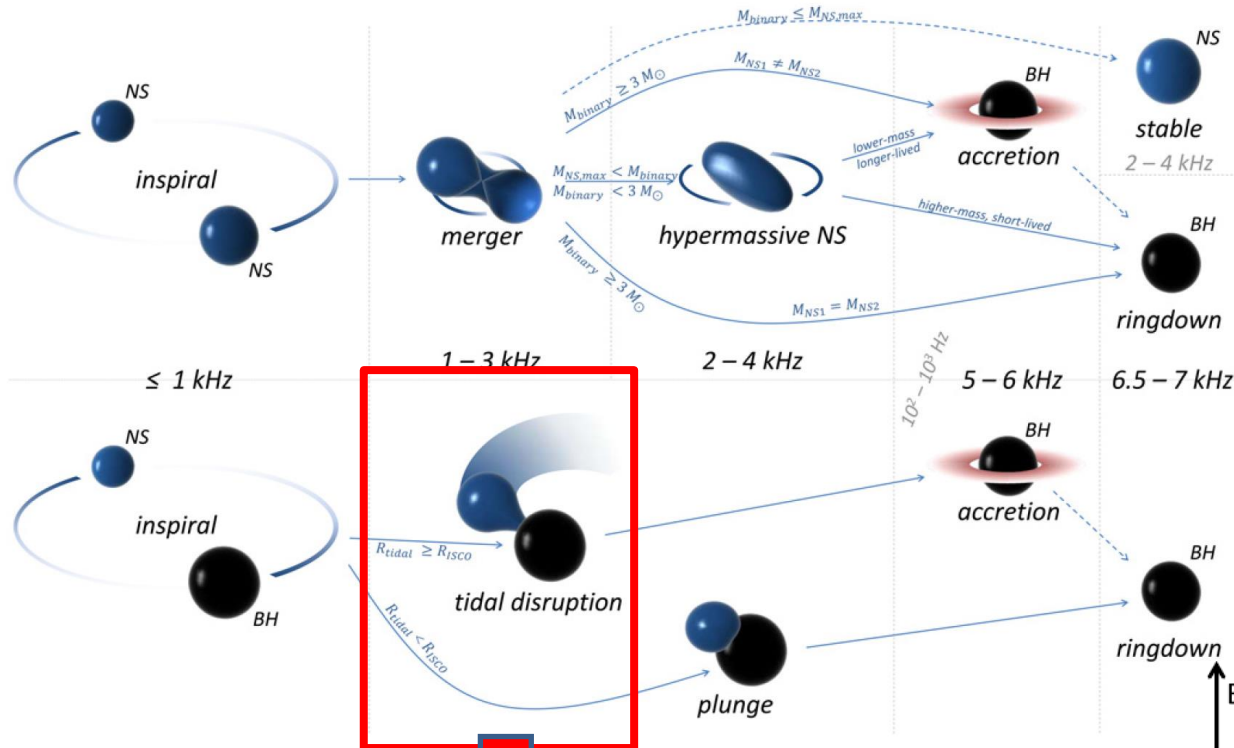


Actual detections

EM emission from NS+BH

Class. Quantum Grav. **30** (2013) 123001

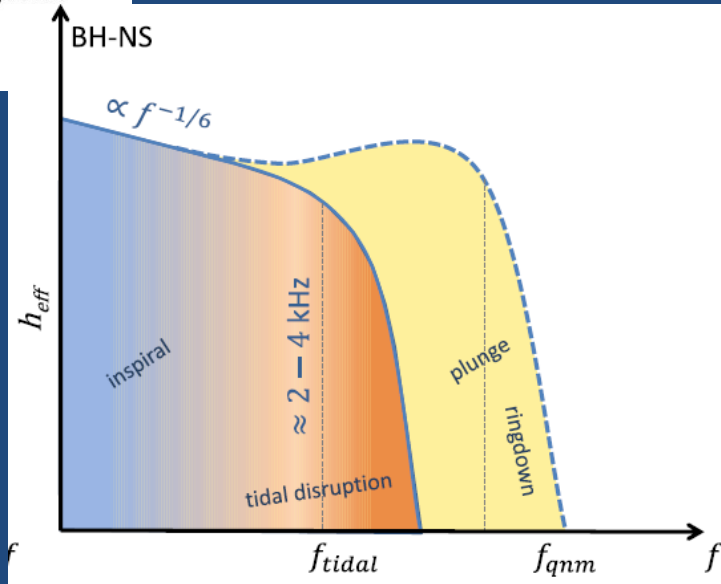
Topical Review



EM-favorable

18.07.2022

Dubna-2022



Mass shedding and tidal disruption

$$r_{\text{ISCO}}/M = 3 + Z_2 \mp \sqrt{(3 - Z_1)(3 + Z_1 + 2Z_2)}$$

$$Z_1 \equiv 1 + (1 - \chi_1^2)^{1/3}$$

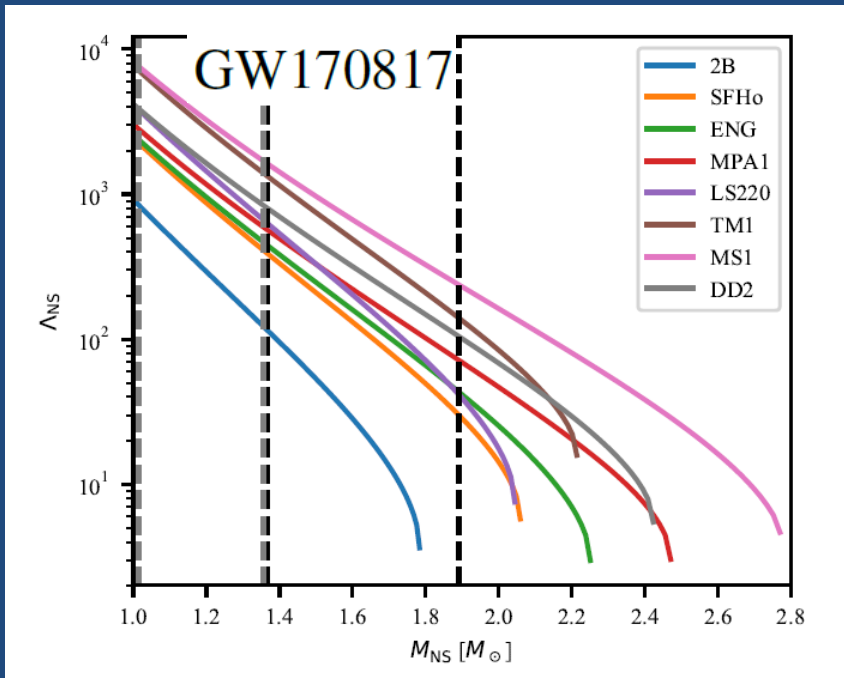
$$\times \left[(1 + \chi_1)^{1/3} + (1 - \chi_1)^{1/3} \right]$$

$$Z_2 \equiv \sqrt{3\chi_1^2 + Z_1^2}$$

- $R_{\text{tid}} \sim R_{\text{ns}} (M_{\text{bh}}/M_{\text{ns}})^{1/3}$
Mass shedding if

$$R_{\text{tid}} > R_{\text{ISCO}}$$

- Depends on NS compactness $C = M_{\text{ns}}/R_{\text{ns}}$ (EOS)
- **Tidal parameter**
 $\Lambda = 2k_2/(3C^5)$
- Depends on the BH spin

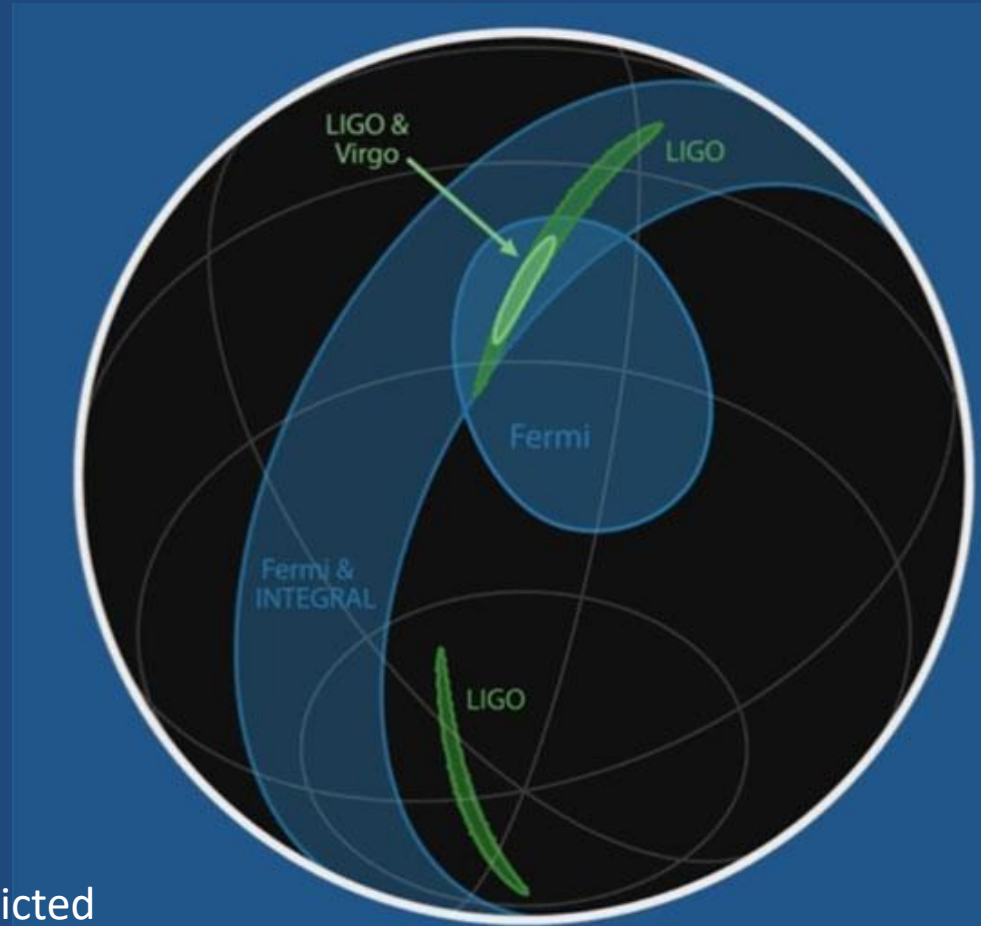
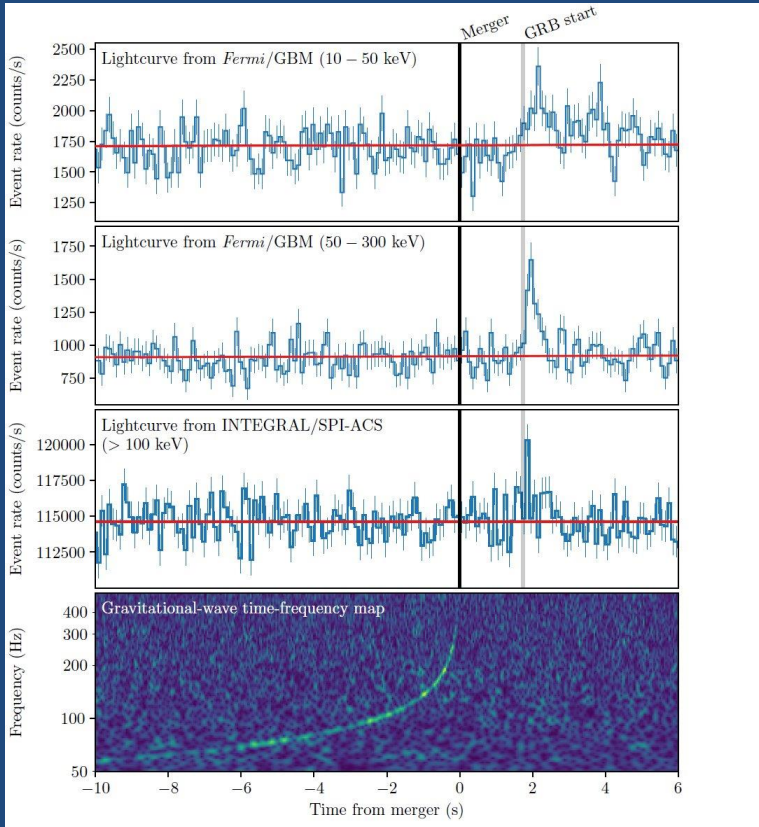


Binary NS and multimessenger astronomy



Image credit: LIGO/Caltech/MIT/Sonoma State (Aurore Simonnet)

GRB170817A and GW170817



GRB association with NS+NS was predicted
by [Blinnikov et al. 1984 SvAL](#)

$$L_{\text{iso}} = (1.6 \pm 0.6) \times 10^{47} \text{ erg s}^{-1}$$

Fundamental inferences

- 1) EM and GW speed:

$$\Delta v/v_{\text{EM}} \approx v_{\text{EM}} \Delta t/D$$

10-s EM delay

$$-3 \times 10^{-15} \leq \frac{\Delta v}{v_{\text{EM}}} \leq +7 \times 10^{-16}$$

Instantaneous, $D > 26$ Mpc

- 2) Equivalence principle

Shapiro delay

$$\delta t_S = -\frac{1 + \gamma}{c^3} \int_{r_e}^{r_o} U(\mathbf{r}(l)) dl$$

MW: $M = 2.5 \times 10^{11} M_{\odot}$
 $R < 100$ kpc

$$-2.6 \times 10^{-7} \leq \gamma_{\text{GW}} - \gamma_{\text{EM}} \leq 1.2 \times 10^{-6}$$

Cf. from Cassini mission: $2.1 \pm 2.3 \times 10^{-5}$

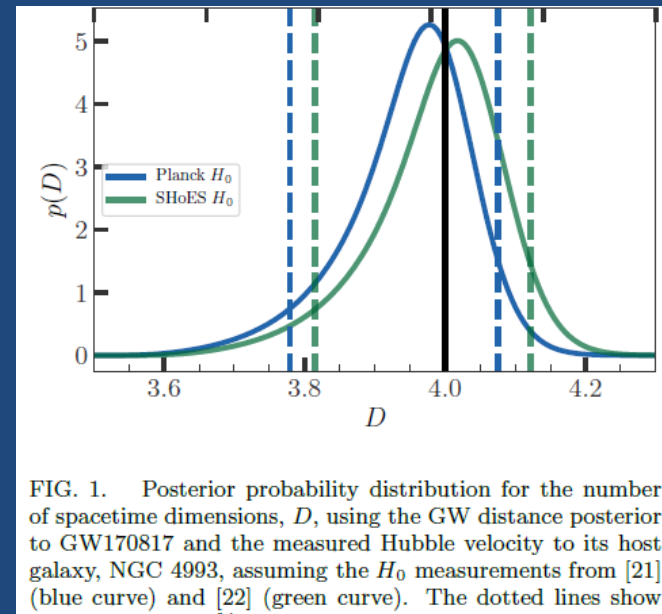
ApJL, 848, L13, 2017

- 3) Number of additional dimensions

$$h \propto \frac{1}{d_L^\gamma}$$

$$\gamma = \frac{D-2}{2}$$

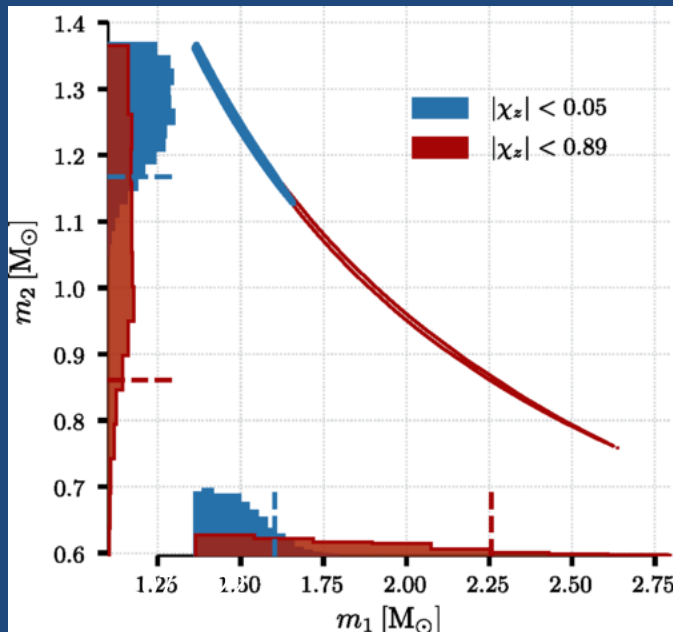
H_0 prior $\text{km s}^{-1} \text{Mpc}^{-1}$	γ	D
$H_0 = 73.24 \pm 1.74$ [22]	$1.01^{+0.04}_{-0.05}$	$4.02^{+0.07}_{-0.10}$
$H_0 = 67.74 \pm 0.46$ [21]	$0.99^{+0.03}_{-0.05}$	$3.98^{+0.07}_{-0.09}$



arXiv:1801.08160

Parameters from GW signal

	Low-spin priors ($ \chi \leq 0.05$)	High-spin priors ($ \chi \leq 0.89$)
Primary mass m_1	1.36–1.60 M_\odot	1.36–2.26 M_\odot
Secondary mass m_2	1.17–1.36 M_\odot	0.86–1.36 M_\odot
Chirp mass \mathcal{M}	1.188 $^{+0.004}_{-0.002}$ M_\odot	1.188 $^{+0.004}_{-0.002}$ M_\odot
Mass ratio m_2/m_1	0.7–1.0	0.4–1.0
Total mass m_{tot}	2.74 $^{+0.04}_{-0.01}$ M_\odot	2.82 $^{+0.47}_{-0.09}$ M_\odot
Radiated energy E_{rad}	$> 0.025 M_\odot c^2$	$> 0.025 M_\odot c^2$
Luminosity distance D_L	40 $^{+8}_{-14}$ Mpc	40 $^{+8}_{-14}$ Mpc
Viewing angle Θ	$\leq 55^\circ$	$\leq 56^\circ$
Using NGC 4993 location	$\leq 28^\circ$	$\leq 28^\circ$
Combined dimensionless tidal deformability $\tilde{\Lambda}$	≤ 800	≤ 700
Dimensionless tidal deformability $\Lambda(1.4M_\odot)$	≤ 800	≤ 1400



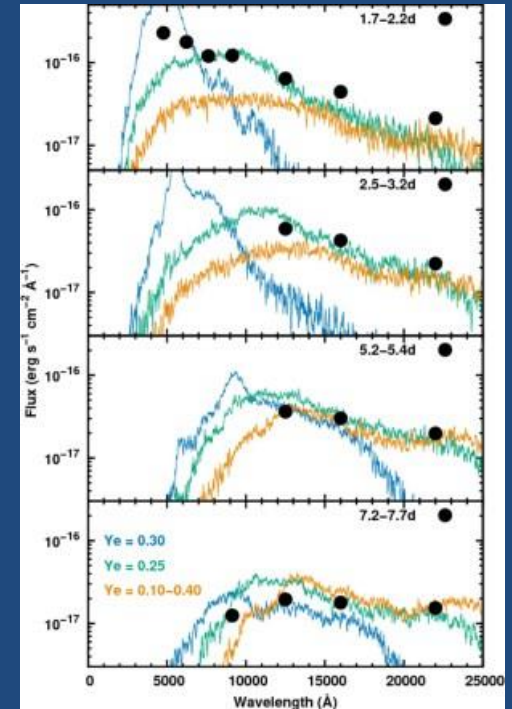
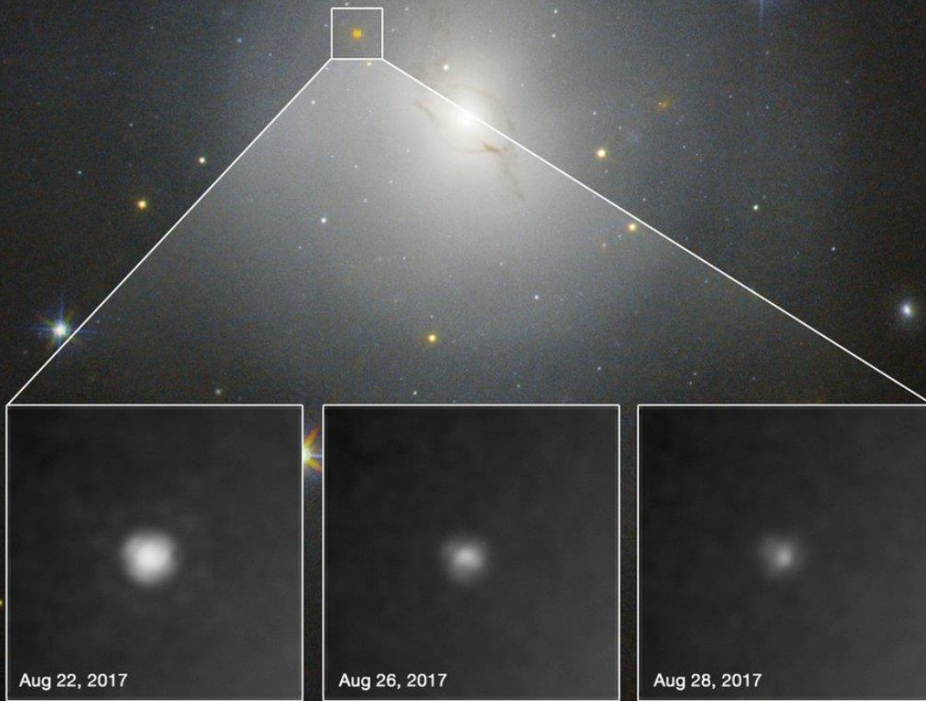
$$\tilde{\Lambda} = \frac{16(m_1 + 12m_2)m_1^4\Lambda_1 + (m_2 + 12m_1)m_2^4\Lambda_2}{(m_1 + m_2)^5}$$

$$H_0 = 70_{-8}^{+12} \text{ km s}^{-1} \text{ Mpc}^{-1}$$

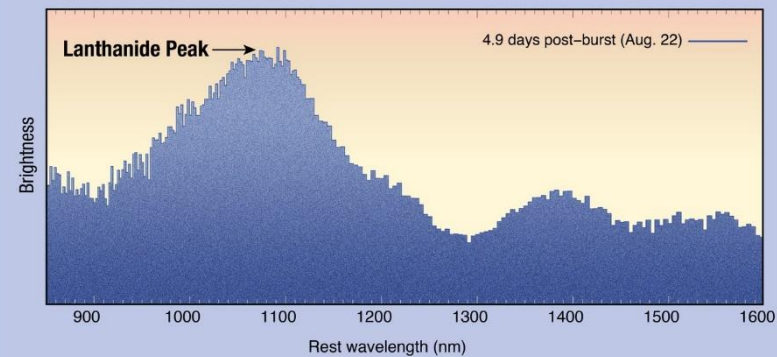
Merging rate $1540_{-1220}^{+3200} \text{ Gpc}^{-3} \text{ yr}^{-1}$

Optical and IR observations of kilonova

NGC 4993
40 Mpc, E/SO



Spectrum of a Kilonova

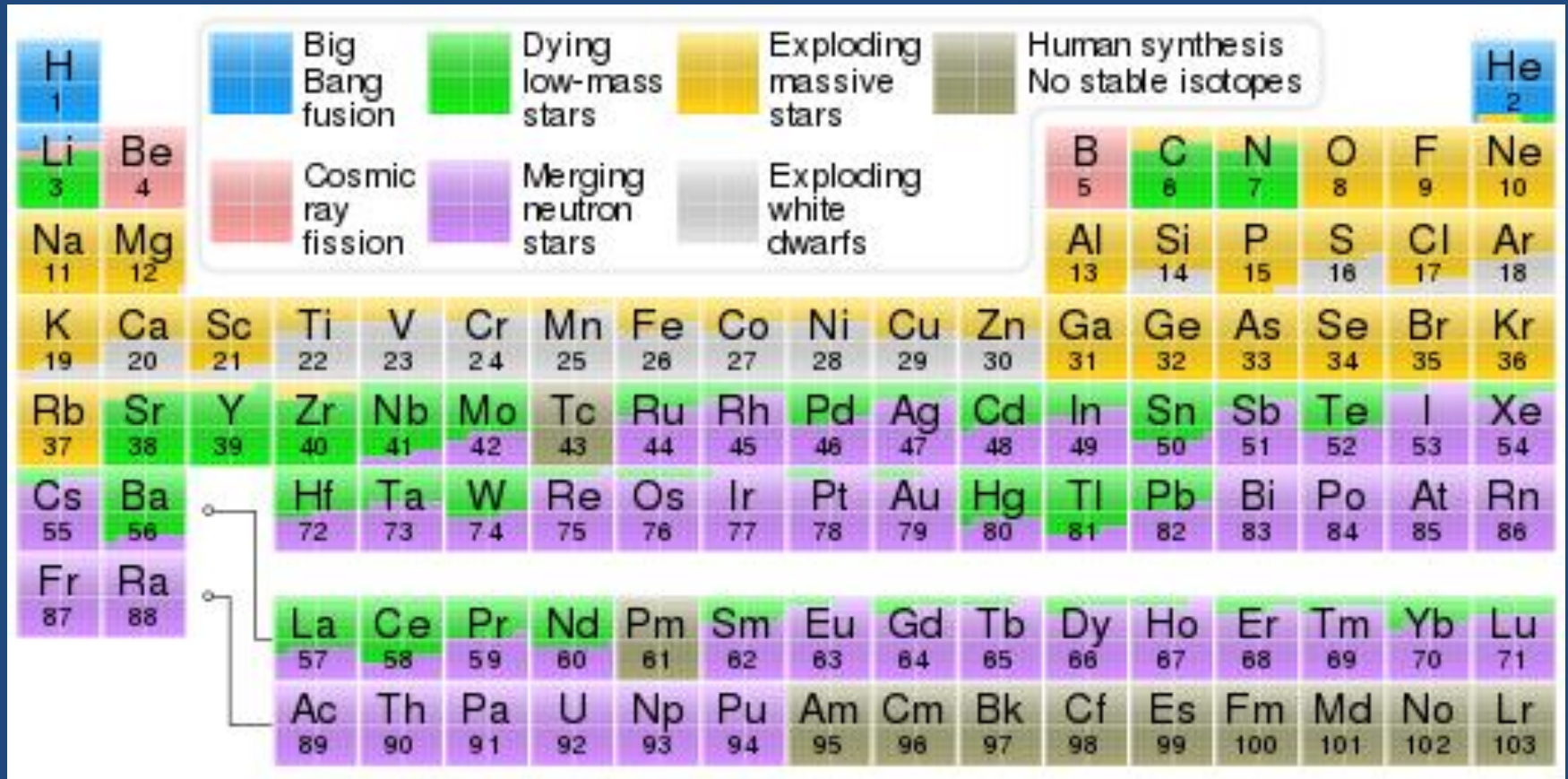


[1710.05850](https://arxiv.org/abs/1710.05850)

1507.2022

Dubna-2022

Binary NS as main production channel for r-elements



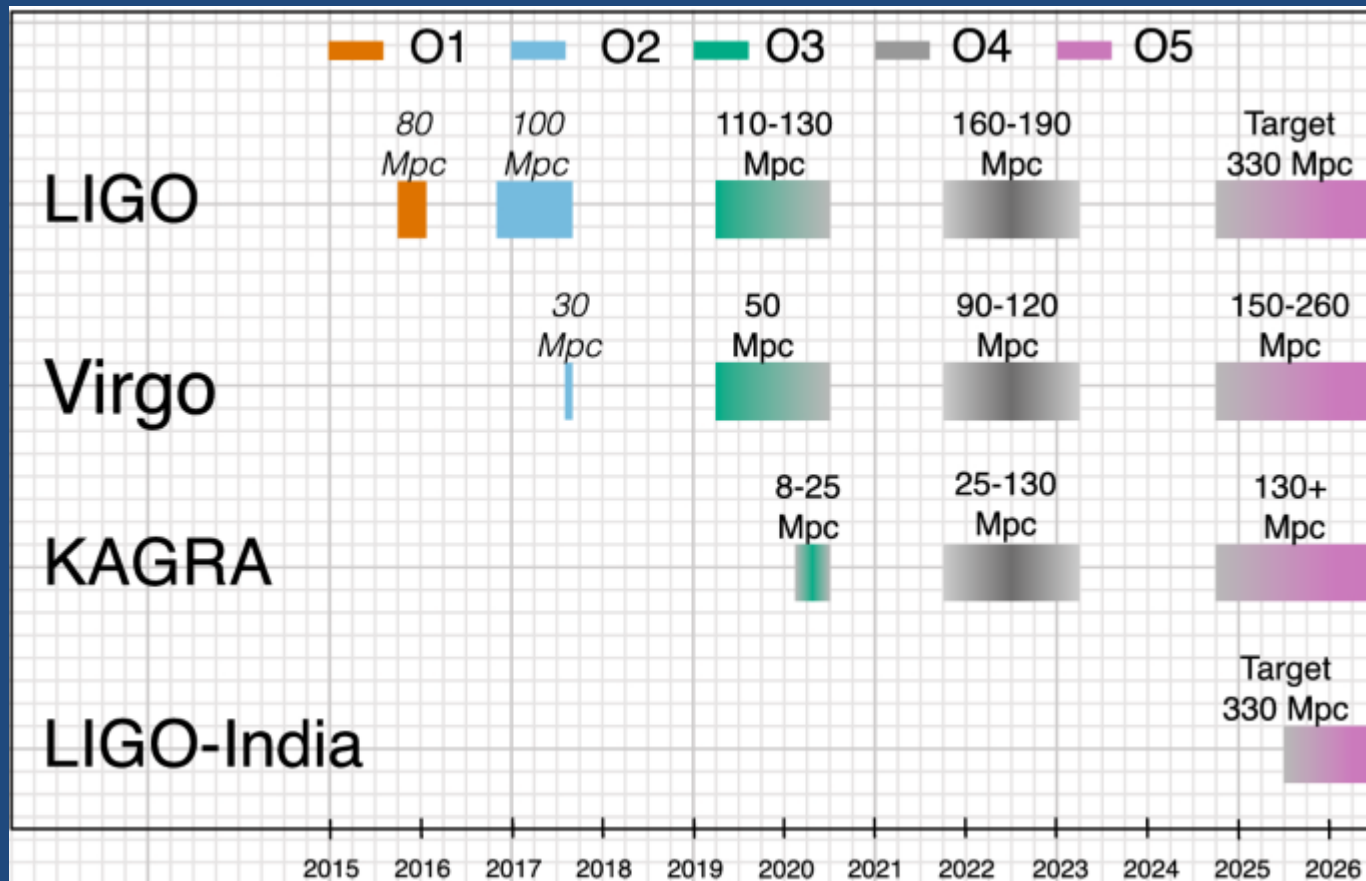
Joint GW+kilonova analysis

Table 1: Key Properties of GW170817

Property	Value	Reference
Chirp mass, \mathcal{M} (rest frame)	$1.188^{+0.004}_{-0.002} M_{\odot}$	1
First NS mass, M_1	$1.36 - 1.60 M_{\odot}$ (90%, low spin prior)	1
Second NS mass, M_2	$1.17 - 1.36 M_{\odot}$ (90%, low spin prior)	1
Total binary mass, $M_{\text{tot}} = M_1 + M_2$	$\approx 2.74^{+0.04}_{-0.01} M_{\odot}$	1
Observer angle relative to binary axis, θ_{obs}	$11 - 33^{\circ}$ (68.3%)	2
Blue KN ejecta ($A_{\text{max}} \lesssim 140$)	$\approx 0.01 - 0.02 M_{\odot}$	e.g., 3,4,5
Red KN ejecta ($A_{\text{max}} \gtrsim 140$)	$\approx 0.04 M_{\odot}$	e.g., 3,5,6
Light r -process yield ($A \lesssim 140$)	$\approx 0.05 - 0.06 M_{\odot}$	
Heavy r -process yield ($A \gtrsim 140$)	$\approx 0.01 M_{\odot}$	
Gold yield	$\sim 100 - 200 M_{\oplus}$	8
Uranium yield	$\sim 30 - 60 M_{\oplus}$	8
Kinetic energy of off-axis GRB jet	$10^{49} - 10^{50}$ erg	e.g., 9, 10, 11, 12
ISM density	$10^{-4} - 10^{-2} \text{ cm}^{-3}$	e.g., 9, 10, 11, 12

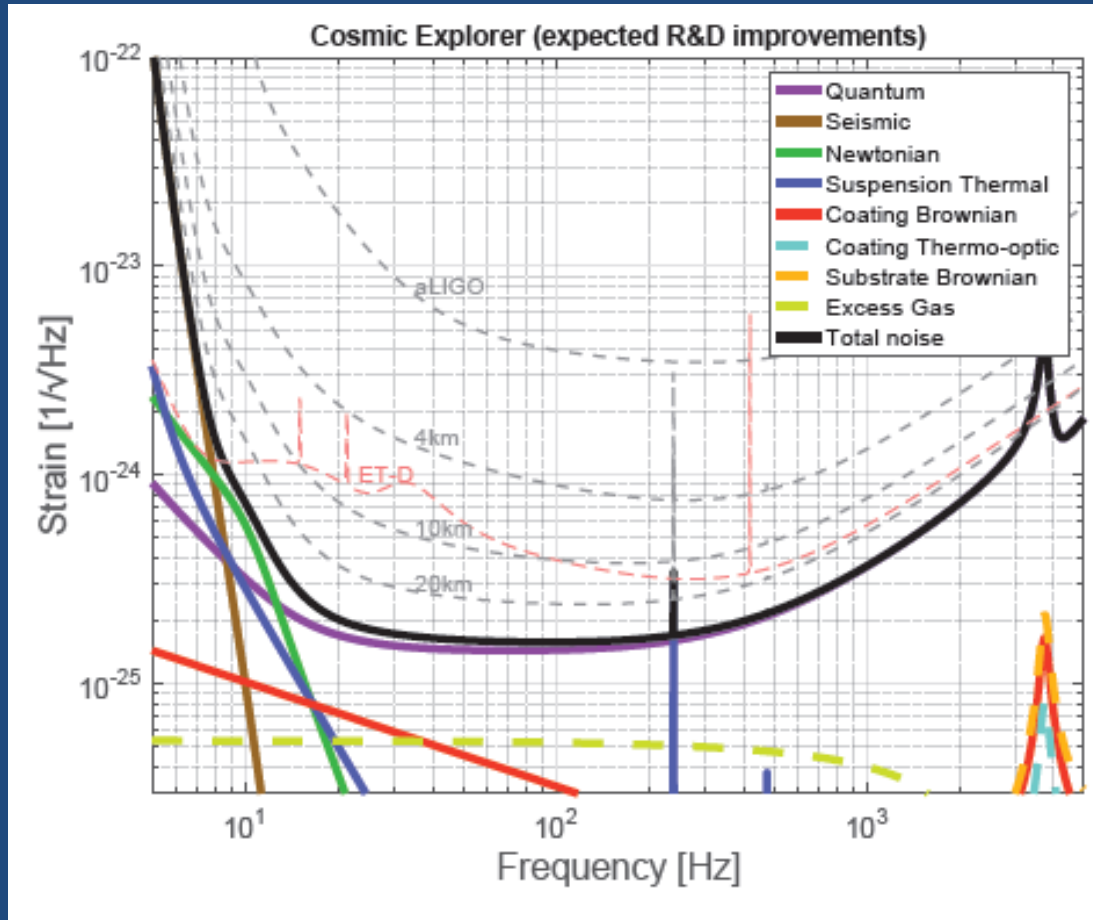
(1) LIGO Scientific Collaboration et al. 2017c; (2) depends on Hubble Constant, LIGO Scientific Collaboration et al. 2017d; (3) Cowperthwaite et al. 2017; (4) Nicholl et al. 2017; (5) Kasen et al. 2017; (6) Chornock et al. 2017; (8) assuming heavy r -process ($A > 140$) yields distributed as solar abundances (Arnoult et al., 2007); (9) Margutti et al. 2017; (10) Troja et al. 2017; (11) Fong et al. 2017; (12) Hallinan et al. 2017

Future prospects (LVK collaboration)



Abbot et al. 2020

40-km LIGO Cosmic Explorer (2035)



Sensitivity of detectors with different lengths.
Solid curves are for a 40km long detector

LIGO Scientific Collaboration, arXiv:1607.08697 [astro-ph.IM]

- LIGO, Virgo, and KAGRA are closely coordinating to start the O4 Observing run together in ~**March 2023**, despite local and global adversities.
- **LIGO** projects a sensitivity goal of **160-190 Mpc** for binary neutron stars. **Virgo** projects a target sensitivity of **80-115 Mpc**. **KAGRA** should be running with greater than **1 Mpc** sensitivity at the beginning of O4, and will work to improve the sensitivity toward the end of O4.

Pulsar timing arrays

- Pulsar timing (Estabrook & Walquist'75, Sazhin'78, Detweiler'79)
- Working collaborations
 - European PTA (EPTA) [42 msPSR]
 - Indian PTA (In PTA)
 - North American Nanohertz Observatory for GW (NANOGrav) [48 msPSR]
 - Parkes PTA (PPTA) [~30 msPSR]
 - >Join into International PTA (IPTA)

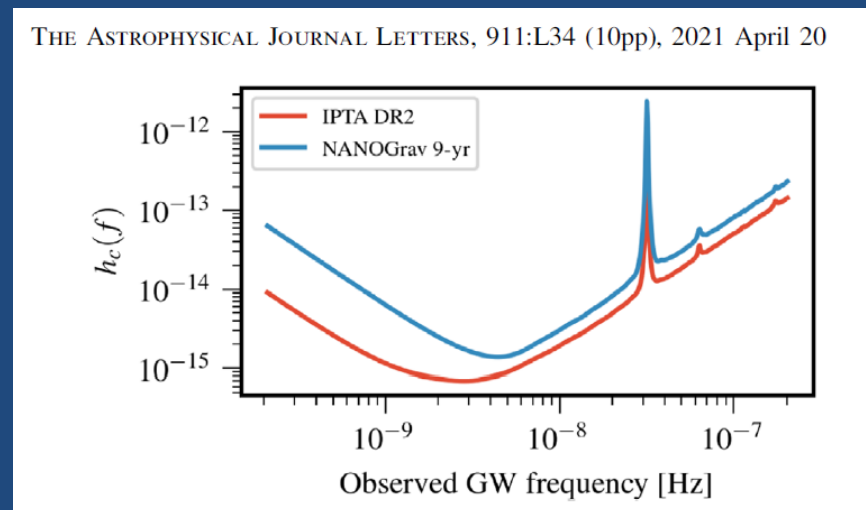
$$R(\text{ns}) \sim 10 (h/10^{-16}) / (f/10^{-8} \text{ Hz})$$

NanoHz GW from PTA observations

- Stochastic GW backgrounds:

$$h_c = A(f/1 \text{ yr}^{-1})^\alpha$$

- Inspiral binary SMBH ($M > 10^7$) (e.g. Sesana+'08, $\alpha = -2/3$)
- Cosmic strings (e.g. Oelmez+'10, $\alpha = -7/6$)
- Cosmological phase transitions, primordial GW (Grishchuk'05 $\alpha = -2$, Lasky+'16 $\alpha = -1$)
- ...



IPTA DR2 results

- Stochastic common spectrum process (CP)

$$h_c = A(f/1 \text{ yr}^{-1})^\alpha$$

$$A = 3.8_{-2.5}^{+6.3} \times 10^{-15}$$

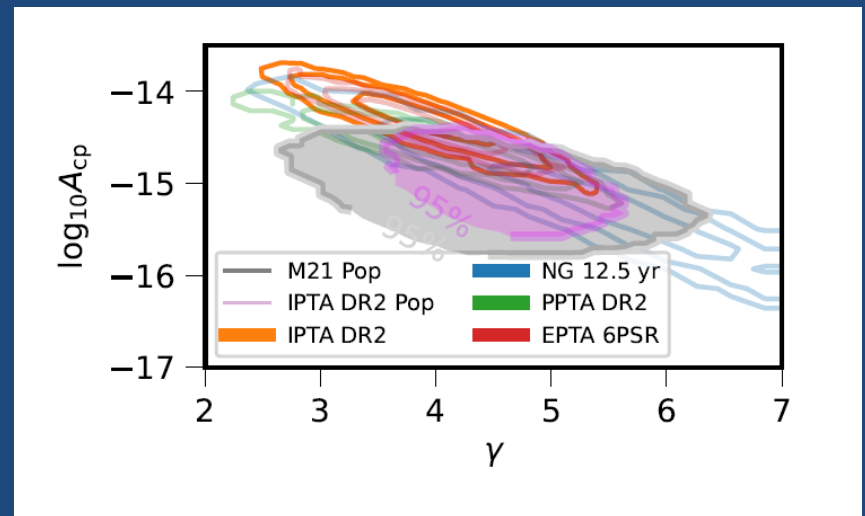
$$\alpha = -0.5 \pm 0.5$$

- Marginally consistent with SMBH GWB ($\alpha=-2/3$) with space density

$$\Phi_0 \approx 10^{-5} \text{ Mpc}^{-3}$$

- Cosmic string tension $\mu G \sim [4-10] \times 10^{-11}$ (Ellis, Lewicki'21)

$$h_c(f) = A_{\text{CP}} \left(\frac{f}{f_{\text{yr}}} \right)^{(3-\gamma_{\text{CP}})/2}$$



$$A_{\text{GWB}}^2 = \frac{4}{3\pi^{1/3}} \iiint dM_1 dz dq \frac{\mathcal{M}^{5/3}}{(1+z)^{1/3}} \frac{d^3 \Phi_{\text{BHB}}}{dM_1 dz dq}$$

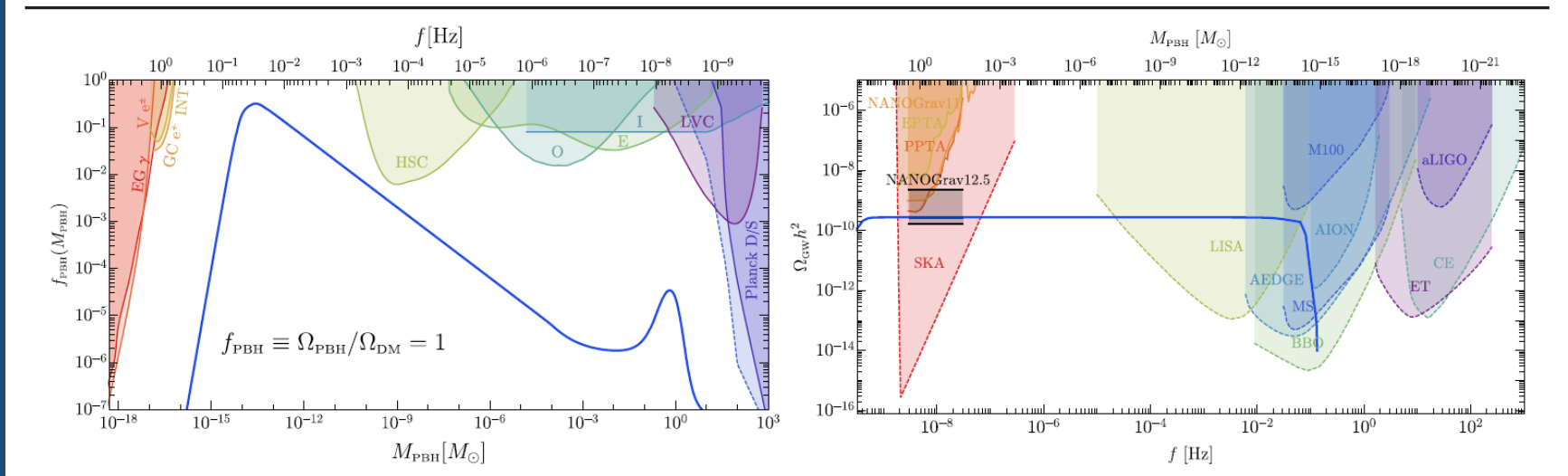
Antoniadis+ 2201.03980

Cosmological inferences if detected

CP signal is GWB

- 2d-order GWs accompanying formation of PBH from collapse of inflationary scalar perturbations

PHYSICAL REVIEW LETTERS **126**, 041303 (2021)



De Luca, Franciolini, Riotto '21

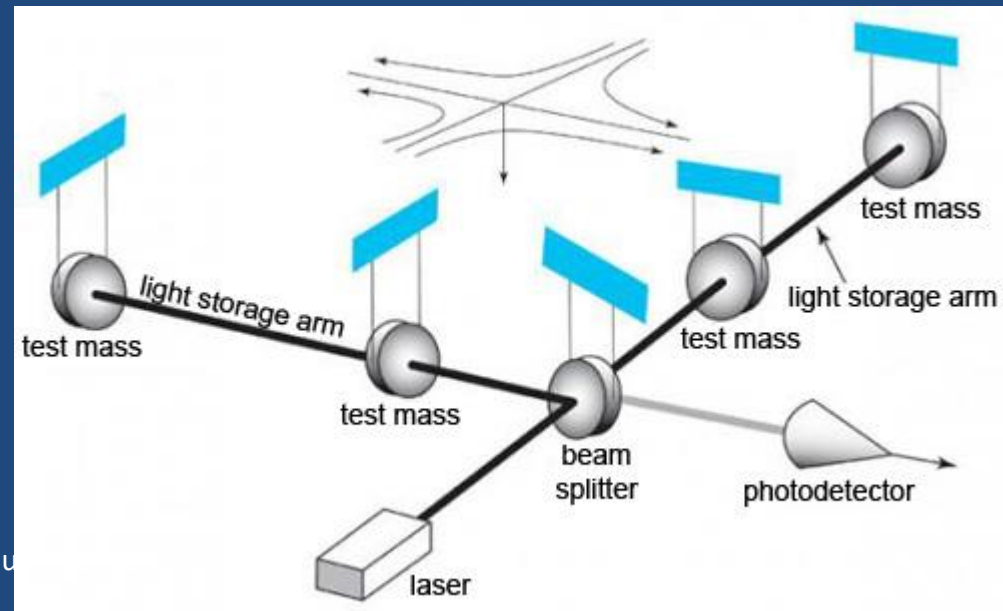
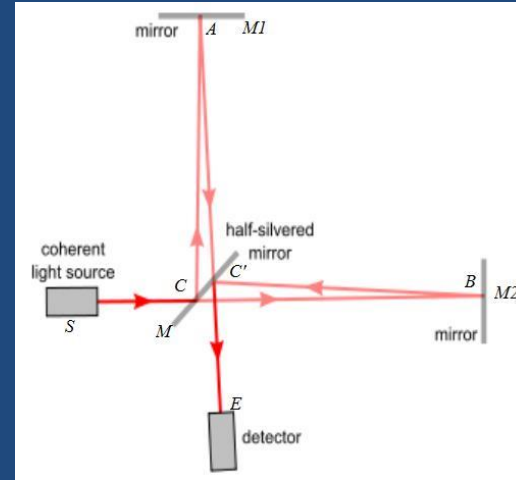
Conclusions

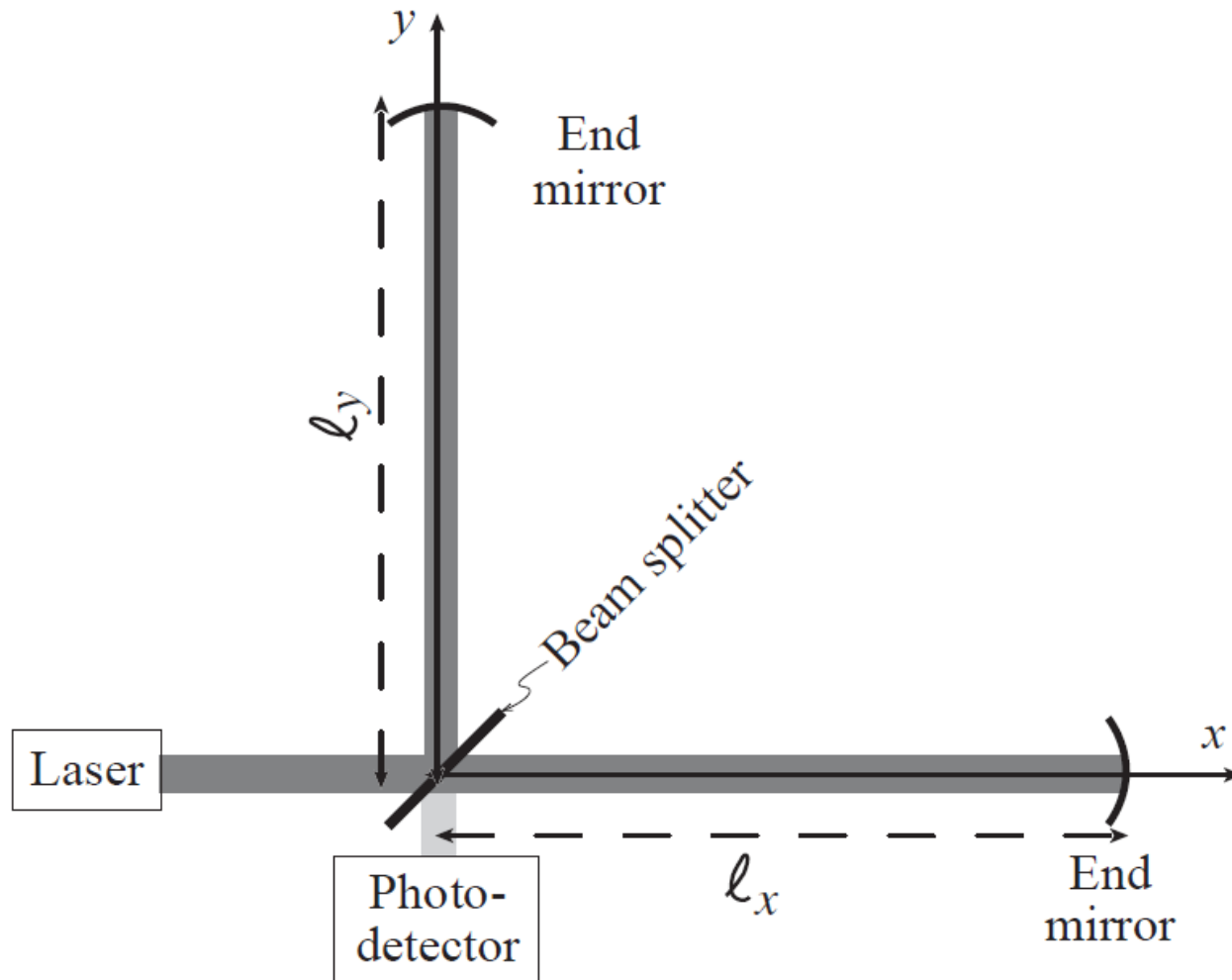
- LVK O1+O2+O3: ~ 100 detections of binary BH and NS mergings, mostly binary BH, rate $\sim 10\text{-}200 \text{ Gpc}^{-3} \text{ yr}^{-1}$
- **Astrophysical problems** in formation of massive BH with $M \sim 100 M_{\odot}$, extreme mass ratio BH+BH inspirals, BH+NS
- Stochastic nanoHz CP signal **is detected** by NANOGrav and IPTA collaborations. If GWB, it may be produced by SMBH binaries $\sim 10^{-5} \text{ Gpc}^{-3}$ or cosmic strings with tension $\mu G \sim 4 \times 10^{-11}$
- **Pulsar timing as a sensitive probe to new theoretical models of nanoHz GWBs!**

Backup slides

How to detect GWs?

- Michelson interferometer
- Laser interferometry
- $h \sim \Delta L/L$





$$ds^2 = -dt^2 + [1 + h_+(t - z)]dx^2 + [1 - h_+(t - z)]dy^2 + dz^2$$

Phase change in interferometer

$$ds^2 = -c^2 dt^2 + [1 + h(t)]dx^2 + [1 - h(t)]dy^2$$

$$ds = 0 \Rightarrow c^2 dt^2 = [1 + h(t)]dx^2 + [1 - h(t)]dy^2$$

$$X, Y : \tau_{X,Y} = \int dt = \frac{1}{c} \int \sqrt{1 \pm h(t)} dx \approx \frac{L}{c} \pm \frac{hL}{c}$$

GW interferometer

$$\delta x = \frac{1}{2} h_+ l_x \quad \delta y = -\frac{1}{2} h_+ l_y$$

Разность фаз в плечах интерферометра

$$\Delta\varphi(t) = \omega_o(2\delta y - 2\delta x) = \omega_o(l_x + l_y)h_+(t)$$

Модуляция интенсивности

$$\Delta I_{\text{PD}}(t) \propto \Delta\varphi(t) = 2\omega_o l h_+(t)$$

$$\Delta\varphi = \frac{4\pi}{\lambda} Lh$$

How to measure tiny displacements?

$$\Delta\Phi = B \frac{hL}{\lambda}, \quad \frac{BL}{c} \leq \frac{1}{2} \left(\frac{1}{f_{GW}} \right) \Rightarrow B_{\max} \approx 400$$

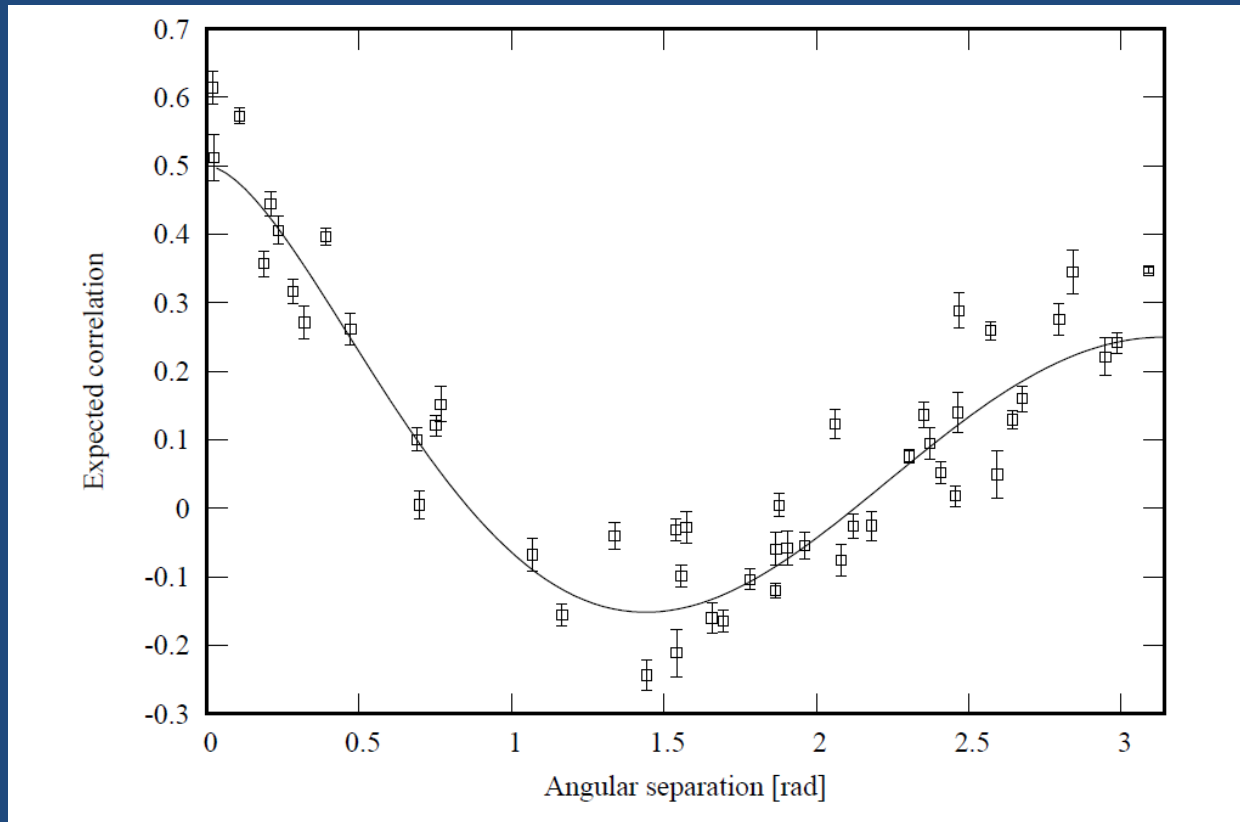
$$\text{Shot noise: } \Delta\Phi_{\min} \sim \frac{1}{\sqrt{N_{ph}}},$$

$$N_{ph} = \frac{P_{laser} \times (\# \text{ recyclings})}{\hbar\omega} \times \Delta t \sim 2 \times 10^{20}$$

$$\text{@ } P = 60W, \quad \Delta t = 10ms$$

$$h_{\min} \sim \frac{\lambda}{BL} \frac{1}{\sqrt{N_{ph}}} = \frac{0.5\mu}{400 \times 4km} \frac{1}{\sqrt{2 \times 10^{20}}} \sim 10^{-22} !$$

Hellings-Downes correlation



$$\langle r_a^*(t)r_b(t) \rangle = 2C(\xi) \int_0^\infty df \frac{S_h(f)}{(2\pi f)^2} 2[1 - \cos(2\pi ft)]$$

$$C(\xi) = \frac{1}{3} \left\{ 1 + \frac{3}{2} (1 - \cos \xi) \left[\ln \left(\frac{1 - \cos \xi}{2} \right) - \frac{1}{6} \right] \right\}$$